Probing magnetic and triplet correlations in spin-split superconductors with magnetic impurities

C.-H. Huang [1,2] A. Skurativska [1] F. S. Bergeret,[3,1] and M. A. Cazalilla [1,4]

[1]*Donostia International Physics Center (DIPC), 20018 Donostia–San Sebastián, Spain*

[2]*Departamento de Polímeros y Materiales Avanzados: Física, Química y Tecnología, Facultad de Ciencias Químicas, Universidad del País Vasco UPV/EHU, 20018 Donostia-San Sebastián, Spain*

[3]*Centro de Física de Materiales (CFM-MPC) Centro Mixto CSIC-UPV/EHU, 20018 Donostia–San Sebastián, Basque Country, Spain*

[4]*IKERBASQUE, Basque Foundation for Science, Plaza Euskadi 5, 48009 Bilbao, Spain*

(Received 21 February 2024; revised 19 May 2024; accepted 22 May 2024; published 3 July 2024)

A superconductor (SC) in proximity to a ferromagnetic insulator (FMI) is predicted to exhibit mixed singlet and triplet correlations. The magnetic proximity effect of FMI spin splits the energy of Bogoliubov excitations and leads to a spin polarization at the surface for superconducting films that are thinner than the superconducting coherence length. In this work, we study manifestations of these phenomena in the properties of a magnetic impurity coupled via Kondo coupling to this FMI/SC system. Using the numerical renormalization group (NRG) method, we compute the properties of the ground state and low-lying excited states of a model that incorporates the Kondo interaction and a Ruderman-Kittel-Kasuya-Yosida (RKKY)-like interaction with the surface spin polarization. Our main finding is an energy splitting of the lowest even fermion-parity states caused by the proximity to the FMI. As the Kondo coupling increases, the splitting grows and saturates to a universal value equal to twice the exchange field of the FMI. We introduce a two-site model that can be solved analytically and provides a qualitative understanding of this and other NRG results. In addition, using perturbation theory, we demonstrate that the mechanism behind the splitting involves the RKKY field and the triplet correlations of the spin-split superconductor. A scaling analysis combined with NRG shows that the splitting can be written as a single-parameter scaling function of the ratio of the Kondo temperature and the superconducting gap, which is also numerically obtained.

DOI: 10.1103/PhysRevResearch.6.033022

I. INTRODUCTION

The search for superconductors with a spin-triplet electron pairing mechanism is an ongoing endeavor motivated by their potential to host unique excitations [1–3] with promising applications to quantum hardware [4,5]. Within this area, one research direction focuses on studying candidate materials where this type of pairing occurs intrinsically [6–8]. Alternatively, triplet correlations can be induced *extrinsically* in, e.g., superconductor-ferromagnet hybrid systems [9], or conventional superconductors in proximity to a ferromagnetic insulator [10].

In a conventional superconductor, Cooper pairs condense in a spin-singlet state. When the condensate interacts with a local exchange field via the proximity effect either to a metallic ferromagnet or ferromagnetic insulator, part of the singlets transforms into triplet pairs. Theoretically, this has been extensively investigated using the quasiclassical approach in Refs. [9,11–15]. In the particular case of a ferromagnetic insulator (FMI)/superconductor (SC) heterostructure, an indirect signature of the induced exchange field and triplet correlations can be observed as a spin splitting of the density of states of thin SC layers, even in the absence of an externally applied field, as confirmed in several experiments [16–18].

The ferromagnet-superconductor interaction can be described by treating the magnetization of the ferromagnet as a classical variable that provides an exchange field at the boundary. On the other hand, the study of magnetic impurities in a superconducting host is a longstanding area of research, with current interest focusing on developing experimental platforms that allow the control and tuning of quantum states of such systems with high accuracy. Advances in scanning tunneling spectroscopy (STS) allow one to probe impurities on the surface of a superconductor with atomic-scale resolution [19–22]. Molecular junctions [23] and superconducting nanowires coupled to a quantum dot [24–29] can be tuned to regimes where they can be modeled as quantum impurities.

Furthermore, chains of magnetic impurities (adatoms) on top of a superconductor have been extensively studied to realize the paradigmatic Kitaev chain [1–3,30–32]. Recently, two nearby magnetic impurities in a superconductor have been proposed to realize an effective two-level system, which is a key ingredient of a qubit, the building block of a quantum computer [33]. Despite the proposals, control of the system parameters remains a major challenge, requiring a deeper understanding of the magnetic interactions between impurities and the substrate. When two impurities are placed on a superconductor, their interaction is mediated by the itinerant electrons, resulting in an effective long-range interaction. Depending on the distance between the

impurities, the Ruderman-Kittel-Kasuya-Yosida (RKKY) interaction [34–36] can be antiferromagnetic [37,38] or even ferromagnetic at distances larger than the coherence length in superconductors with strong spin-orbit coupling [39]. Some recent proposals have also discussed tuning magnetic interactions by applying microwave fields [40] or by varying the orientation of an external magnetic field [41]. In this regard, it is interesting to explore the possibility of manipulating the magnetic interaction between impurities through an effective exchange field generated via the proximity to an FMI/SC system at zero external magnetic field. The first step in this direction is to study how the exchange field affects the ground state and the spectral properties of a single impurity.

In this work, we address this question by analyzing a FMI/SC heterostructure coupled to a spin-$\frac{1}{2}$ magnetic impurity. Such a system can be seen as a platform to study the interplay between triplet correlations and the magnetic interactions induced by the FMI. As mentioned above, an FMI in proximity to an SC leads to spin polarization of the quasiparticle states, resulting in spin splitting of the coherence peaks in the density of states [16,18]. To capture this effect, we introduce an effective homogeneous exchange field h that couples to the electronic states described by the BCS mean-field Hamiltonian as a Zeeman coupling. This is justified by assuming that the thickness of the superconducting layer is smaller than the superconducting coherence length. This effective h drastically modifies the exchange interaction between the impurity spin and the electrons in the SC. In addition, Cooper pairs in the SC mediate an effective RKKY-like interaction between the impurity spin and the FMI.

After introducing the model, we describe the results obtained by solving it with the numerical renormalization group (NRG) method [42–46] for the ground state and the low-lying energy spectrum. In the absence of the FMI, the ground-state properties of a superconductor/impurity system have been studied extensively [47]. It was found that as the (Kondo) exchange coupling with the impurity grows, the system undergoes a quantum phase transition where the fermion parity of the ground state changes from an even-parity doublet to an odd-parity singlet state. Our main finding in this work is that the presence of an exchange field induced by proximity to the FMI lifts the spin degeneracy of the even-parity doublet. The spin splitting of the doublet exists for any finite value of the Kondo coupling. Furthermore, in the weak-coupling regime, we find a shift of the threshold for continuum excitations only for electrons tunneling with spin antiparallel to the ground-state spin. Previously, Ref. [48] addressed the problem of a quantum impurity coupled to a spin-split superconductor using NRG. Similarly to this work, a splitting of the doublet states was observed. However, in the model of Ref. [48], this effect requires an in-plane external magnetic field, which equally splits all electronic bands, while in our system, the splitting stems from the proximity to FMI and affects only electrons in the superconductor in a narrow energy window around the Fermi energy.

Moreover, although the results obtained using NRG are quantitatively accurate, they do not provide an intuitive picture of the underlying mechanisms leading to the splitting of the doublet and the shift of the threshold for the continuum of single-particle excitations. Thus, to gain a qualitative understanding, we introduce a minimal two-site model based on zero-bandwidth approximation [22,49] that captures the essence of the NRG results. Furthermore, in the limit of weak Kondo coupling, we use perturbation theory to analytically calculate the splitting. We find that the first-order energy correction comes from the effective RKKY-like interaction between the FMI and the impurity, while the second-order contribution originates from triplet correlations present in an FMI/SC substrate.

The findings described above have direct consequences for the excitation spectrum causing a spin splitting of the lowest-energy single-particle excitations, namely, the Yu-Shiba-Rusinov (YSR) excitations [50–52] in the strong-coupling regime of the magnetic impurity. This splitting can be measured using tunneling probes on, e.g., a quantum dot coupled to an FMI/SC nanowire or a magnetic adatom on the surface of the FMI/SC heterostructure.

The rest of the article is organized as follows: In Sec. II, we introduce the many-body Hamiltonian describing the system under study. In Sec. III, we describe the results of the NRG calculations of the ground state and the low-energy excitations. In Sec. IV, we introduce a minimal two-site model that qualitatively reproduces the key features of the results obtained using NRG. In Sec. V, we describe the results of perturbation theory applied to a two-site model and an extended superconductor in the limit of weak Kondo coupling. In Sec. VI, we describe the effect of the exchange field on other spectral features in the continuum part of the tunneling spectrum. Unless otherwise stated, we will work in units where $\hbar = 1$.

II. MODEL

We consider a superconductor/ferromagnetic-insulator (FMI/SC) heterostructure coupled to a spin-$\frac{1}{2}$ magnetic impurity via an isotropic antiferromagnetic (Kondo) exchange interaction. We introduce the following Hamiltonian to describe the system:

$$H = H_0 + H_K + H_{\mathrm{RKKY}}, \tag{1}$$

$$H_0 = \sum_{k\sigma} \epsilon_k c^\dagger_{k\sigma} c_{k\sigma} + h \sum_{k,\sigma\sigma'} \left[c^\dagger_{k\sigma} \left(2s^z_{\sigma\sigma'}\right) c_{k\sigma'}\right] + \Delta \sum_k [c^\dagger_{k\downarrow} c^\dagger_{-k\uparrow} + c_{k\downarrow} c_{-k\uparrow}], \tag{2}$$

$$H_K = J\boldsymbol{S}\cdot\boldsymbol{s}_0, \tag{3}$$

$$H_{\mathrm{RKKY}} = J\rho_0 h S^z. \tag{4}$$

Here, $c_{k\sigma}$ ($c^\dagger_{k\sigma}$) is the annihilation (creation) operator for the electrons in the superconductor.

In Eq. (1), H_0 describes the FMI/SC heterostructure in the absence of magnetic impurity. Δ is the strength of the pairing potential. Proximity to an FMI gives rise to an exchange field h in the SC that couples to the electron spin as a Zeeman field and therefore splits the Bogoliubov quasiparticle bands [17,53]. However, unlike the Zeeman coupling to a uniform magnetic field that equally splits all electronic bands, the effective exchange field stems from the magnetic proximity effect, and hence only splits the bands in an energy shell

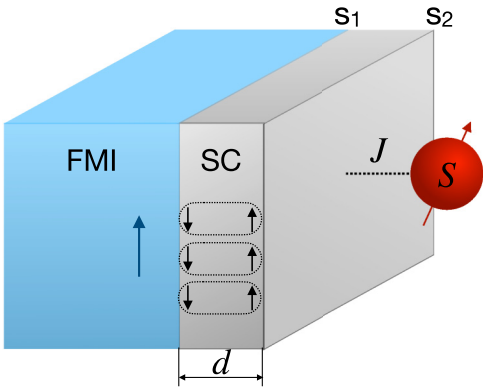

FIG. 1. Schematic representation of an FMI/SC heterostructure coupled to an impurity spin $\boldsymbol{S}$ via a (Kondo) exchange coupling of amplitude J. The superconducting layer has a thickness of $d \ll \xi$ (but larger than the electron mean free path), with ξ the superconducting coherence length. The FMI gives rise to the spin splitting of the quasiparticle density of states in the SC and induces opposite spin polarization on the two superconducting interfaces S_1 and S_2, i.e., $\mathcal{P}(S_1) = -\mathcal{P}(S_2)$. This results in an effective RKKY-type interaction between the FMI and the impurity spin. The blue arrow indicates the orientation of the average magnetic moment in the FMI.

around the Fermi energy for which pairing correlations are important [12,13] (in conventional SCs, for excitation energy $\lesssim \omega_D$, ω_D being the Debye frequency).

In most experiments where spin splitting has been observed [16–18], superconducting films, such as those made of aluminum, are used. These films have a thickness d greater than the typical elastic mean free path ℓ, but smaller than the superconducting coherence length ξ. In this case, the exchange field at distances greater than ℓ from the FMI/SC interface can be considered homogeneous and proportional to $1/d$ [13,54]. From the mean-field perspective, the proximity-induced exchange field h plays a role akin to the superconducting pairing potential. For simplicity, in Eq. (1) we choose h to be oriented along the z axis.

H_K describes an isotropic Kondo coupling between the impurity spin and the spin of the electrons in a superconductor, where J is the exchange coupling, $\boldsymbol{S}$ the spin of the magnetic impurity, and $\boldsymbol{s}_0$ is the spin density of the superconductor at the position of the impurity, i.e., $\boldsymbol{s}_0 = (1/\Omega)\sum_{\boldsymbol{k}\boldsymbol{k}'} c^\dagger_{\boldsymbol{k}\sigma}\boldsymbol{s}_{\sigma\sigma'}c_{\boldsymbol{k}'\sigma'}$, where $\boldsymbol{s} = \boldsymbol{\sigma}/2$ are (half) the spin Pauli matrices and Ω the system volume. The energy scales that determine the existence of a magnetic moment at the impurity and its interaction with the host electrons are the intraorbital Coulomb energy U and the orbital energy ϵ_d, which are typically much larger than ω_D. Between U and ω_D, pairing fluctuations are negligible and the electronic states are not spin split by the proximity to the FMI. Therefore, at the scale where the pairing and exchange potentials set in, the Kondo coupling can be considered spin isotropic.

However, proximity to the FMI modifies the interaction of the impurity spin with the superconductor by giving rise to an effective RKKY-type interaction described by H_{RKKY} in Eq. (1). In the presence of the FMI, the superconductor is locally polarized at the interface S_1 (see Fig. 1). Since the impurity is located at the interface S_2, at a distance d ($d \ll \xi$ but $d \gg \ell$) to the FMI, the surface S_2 exhibits opposite spin polarization due to pairing correlations (see Fig. 1). Therefore, an RKKY exchange field emerges at the interface S_2, which is modeled by $H_{\mathrm{RKKY}} = J\langle\boldsymbol{s}\rangle_{S_2}\cdot\boldsymbol{S}$, where $\langle\boldsymbol{s}\rangle_{S_2}$ is the polarization at S_2 and it is estimated to leading order as the Pauli susceptibility [55–58], i.e., $\langle\boldsymbol{s}\rangle_{S_2} = -\langle\boldsymbol{s}\rangle_{S_1} = \chi_S\boldsymbol{h} \simeq \rho_0\boldsymbol{h}$, where $\boldsymbol{h} = h\boldsymbol{e}_z$, χ_S is the spin susceptibility, and ρ_0 is the density of state at the Fermi surface.

Taking into account all these considerations and neglecting any weak scattering potential that breaks particle-hole symmetry, the total Hamiltonian describing the system is given by Eq. (1). We stress that it is implicitly understood that this model is an effective description of a magnetic impurity at the surface of the FMI/SC system at energy scales $\approx \omega_D$ or lower. The eigenstates of this model Hamiltonian can be labeled by the z component of the total spin, i.e., $S^z_T = S^z + \sum_{\boldsymbol{k},\sigma\sigma'} c^\dagger_{\boldsymbol{k}\sigma}s^z_{\sigma\sigma'}c_{\boldsymbol{k}'\sigma'}$, and the fermion-parity operator. The latter is defined as $P = \prod_{\boldsymbol{k},\sigma}(-1)^{n_{\boldsymbol{k}\sigma}}$, where $n_{\boldsymbol{k}\sigma} = c^\dagger_{\boldsymbol{k}\sigma}c_{\boldsymbol{k}\sigma}$.

In the absence of the FMI, i.e., for $h = 0$ and $H_{\mathrm{RKKY}} = 0$, this model has been extensively studied in the past and its ground-state and low-lying excitation spectra are fairly well understood [47,50–52]: As a function of the exchange coupling J, the many-body ground state undergoes a (level-crossing) phase transition from a doublet at $J < J_{\mathrm{cr}}$ (weak-coupling regime) to a Kondo singlet ground state at $J > J_{\mathrm{cr}}$ (strong-coupling regime). At $J < J_{\mathrm{cr}}$, the impurity spin is weakly coupled to the electrons in a superconductor and the ground state of the system is a twofold degenerate *doublet* state that is well approximated as a product state of the BCS ground state and the impurity-spin states, i.e., $|\mathrm{BCS}\rangle|\pm 1/2\rangle$. Thus, in the weak-coupling limit, the ground-state doublet has even parity and its total spin is equal to the impurity spin, i.e., $\langle S^z_T\rangle = \langle S^z\rangle = \pm 1/2$. As the exchange coupling J increases, the spin of the impurity couples more strongly to the local spin fluctuations in the superconductor. Eventually, for $J > J_{\mathrm{cr}}$, the ground-state energy is lowered by forming a collective singlet bound state (i.e., $\langle S^z_T\rangle = 0$) consisting of the impurity spin and a polarization cloud of quasiparticle excitations from the superconductor. In the strong-coupling limit, the ground state has odd fermion parity and it is a singlet [43–45,47].

When the single-particle excitation spectrum is probed by a tunneling probe, the spectrum displays a pair of narrow peaks at subgap energies symmetrically around zero bias (i.e., $E = 0$). They correspond to the excitations known as the Yu-Shiba-Rusinov (YSR) states [50–52] and can be excited by a single tunneling electron for $E > 0$ (or hole for $E < 0$). The tunneling of electrons or holes couples states of different fermion parity. Indeed, YSR excitations have previously been described as eigenstates of the Bogoliubov–de Gennes equations obtained from the quadratic Hamiltonian that results after replacing the impurity-spin operator with a classical vector. However, this classical description neglects quantum fluctuations of the impurity spin [43,43,59] and important many-body effects related to, e.g., the parity of the ground state [22,43,44,60] or the spin of the YSR excitations [61].

Placing a thin superconducting layer in proximity to the FMI brings about new features that are not encountered in conventional SCs. The exchange field h induced

in the superconductor via the magnetic proximity effect generates superconducting correlations in the triplet state, which are "odd" in the Matsubara frequency and are not present when $h = 0$ [9]. Here, we investigate how triplet correlations affect the properties of the magnetic impurity.

Below, we argue that the existence of the triplet correlations has important consequences for the low-lying spectrum of the system described by Eq. (1). Indeed, even if the stability of the (spin-split) superconductor requires $|h| < \Delta$, the exchange field cannot be treated as a weak perturbation. It substantially alters the quasiparticle spectrum below the energy scale for which superconducting correlations are important ($\approx \omega_D$), and we need to treat its effects using a nonperturbative method. This is accomplished by using the numerical renormalization group (NRG) and the results are described in the following section.

III. NRG RESULTS

In this section, we solve the model in Eq. (1) using the numerical renormalization group (NRG) method [42–46].

Tunneling probes such as the scanning tunneling microscope (STM) can access the single-particle spectrum of the system. The tunneling current is proportional to the convolution of the spectral function of the system with that of the tunneling probe (e.g., the tip of the STM). The definition and calculation using NRG of the spectral function, $A_\sigma(\omega)$, are described below in Sec. VI and in Appendix E. Here, we shall simply outline the key results.

Figure 2(a) shows the evolution with the Kondo coupling J of the singlet (in black) and doublet (in blue and red) excitation energies taking the strength of the pairing potential in Eq. (1) to be $\Delta = 10^{-2}D$, where $D \simeq \omega_D$ is the energy cutoff or bandwidth of the model. As the exchange coupling grows, the level-crossing quantum phase transition takes place at $J/\Delta \simeq 40$. At $J = 0$, the ground state is a doublet with $S^z_T = \pm 1/2$, while the lowest-in-energy excited state with $S^z_T = 0$ and the energy approaching $\Delta - h$ is a singlet. The energy of the singlet state as $J \to 0$ can be *qualitatively* explained using the single-site approximation of this system (see Refs. [61,62]).

In the weak-coupling regime, the degeneracy of the ground state is lifted, giving rise to the splitting of the doublet states. For small values of J, the splitting is linear in both J and h (see inset of Fig. 3). This behavior is well reproduced by the leading-order perturbation theory, as discussed in Sec. V. Within perturbation theory, the splitting is given by $\delta E_0/h = J\rho_0 + (J\rho_0)^2 c + O(J^3)$, where c depends logarithmically on the bandwidth D and the gap Δ. The first-order term stems solely from the RKKY interaction and the second-order term is due to the triplet correlations built in the spin-split superconductor. Qualitatively, all of these features at strong and weak coupling are also captured by the minimal two-site model introduced in Sec. IV.

Figure 2(b) shows the evolution of the spectral weight of the YSR peaks in the spectral function. Notice that in the weak-coupling regime for $h \neq 0$, the absolute ground state has total spin $S^z_T = -\frac{1}{2}$ [see Fig. 2(a)]. Since a tunneling electron (hole) can only couple states of the opposite fermion parity, in the weak-coupling regime *at zero temperature*, the YSR excitation is only due to the transition from the spin-down even-parity ground state to the singlet state. On the other hand, in the strong-coupling regime, the ground state is the odd-parity singlet, and therefore the YSR corresponds to excitations to the two low-lying states of even-parity states, which are split by the exchange field h. As a consequence, while the spin-down spectral weight (red line) is continuous across the transition, the spin-up spectral weight (blue line) is nonzero only in the strong-coupling regime. In all cases, it is also worth pointing out, as already noticed in Ref. [61], that the YSR states exhibit a robust spin polarization.

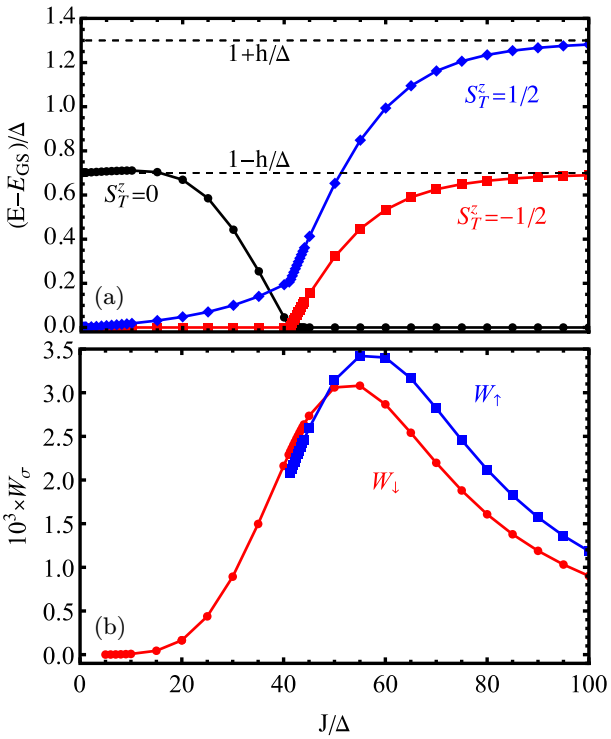

FIG. 2. (a) Energies of the low-lying states of the Hamiltonian, given by Eq. (1), as a function of exchange coupling J in the presence of exchange field, $h = 0.3\Delta$. The black line corresponds to the subgap singlet state extracted from the position of YSR peaks in the spectral functions in weak coupling and the NRG spectrums in strong coupling. The blue and red lines are the doublet states split by the exchange field. Their energies are obtained from the NRG spectrum in the weak-coupling limit and from the spectral functions in the strong-coupling regime. In the weak-coupling limit, the singlet states merge into the shifted continuum at $\Delta - h$, which can be understood using the single-site model [61]. (b) Spectral weights of the YSR excitations as a function of exchange coupling. The blue and red lines are the spin-resolved spectral weights of the spin-up and -down components at the exchange field, $h = 0.3\Delta$.

IV. TWO-SITE MODEL

NRG provides a quantitatively accurate description of the low-lying states and single-particle spectrum of the model in Eq. (1). However, it does not shed much light on the physical origin of various spectral features. In this section, we show that some understanding of the latter can be obtained by

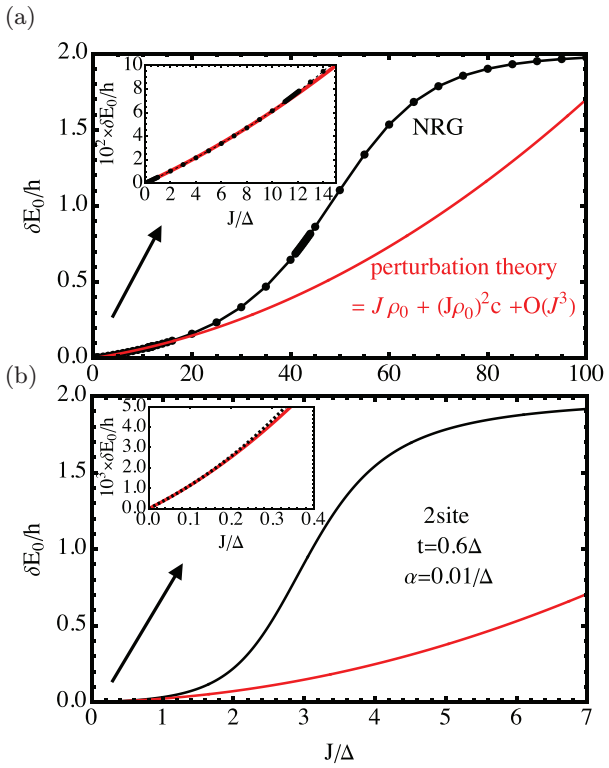

FIG. 3. Ratio of the energy splitting of the two low-lying even-parity states δE_0 to the strength exchange field h as a function of Kondo coupling J obtained via (a) NRG and (b) the minimal two-site model of Eq. (5). In the weak-coupling regime, the splitting is well reproduced by a linear + quadratic law derived using perturbation theory (red curves). For the NRG, the nonuniversal constant $c \simeq 4.43$ is obtained by curve fitting. Parameters used for the NRG calculations: $D = 1$, $\Delta = 0.01D$, $h = 0.3\Delta$. Parameters used for the two-site model: $\Delta = 0.2$, $t = 0.6\Delta$, $h = 0.3\Delta$.

studying a minimal model consisting of a magnetic impurity coupled to two superconducting sites. Previously, Ref. [61] modeled a spin-$\frac{1}{2}$ magnetic impurity coupled to the FMI/SC heterostructure using a single-site model. In this model, the spin-split superconductor is described by a single fermion site coupled to a spin-$\frac{1}{2}$ impurity. Although this model correctly predicts that the YSR states are spin polarized, it cannot describe the variation of the spin splitting with J that is observed in the NRG calculations [see Fig. 2(a)]. In the following, we show that a minimal model capturing this and other effects obtained using NRG necessarily requires two sites to describe the spin-split superconductor. In addition, we demonstrate that the splitting is the consequence of the magnetic RKKY interaction and the existence of spin-triplet correlations in the spin-split superconductor [63].

In the strong-coupling regime, the splitting of the lowest-lying even-parity states approaches twice the exchange energy, $2h$ [see Fig. 3(a)]. It may appear as counterintuitive that strongly coupled impurity is sensitive to the exchange field. However, as shown by the NRG method and confirmed by the two-site model introduced below, in the strong-coupling regime, the system exhibits a pair of spin-split single-particle excitations that corresponds to the YSR peaks of the spectral function [cf. Figs. 4(c)–4(e)].

A. Description of the model

Without further ado, let us introduce a two-site model that describes the spin-split superconductor as two sites with the same s-wave pairing ($\propto \Delta$) and exchange ($\propto h$) potentials. Tunneling of the electrons between the two sites with amplitude t is also allowed. The impurity spin $\boldsymbol{S}$ is coupled via Kondo coupling J to the spin of the electrons on one of the two superconducting sites described by $\boldsymbol{s}_0$. The

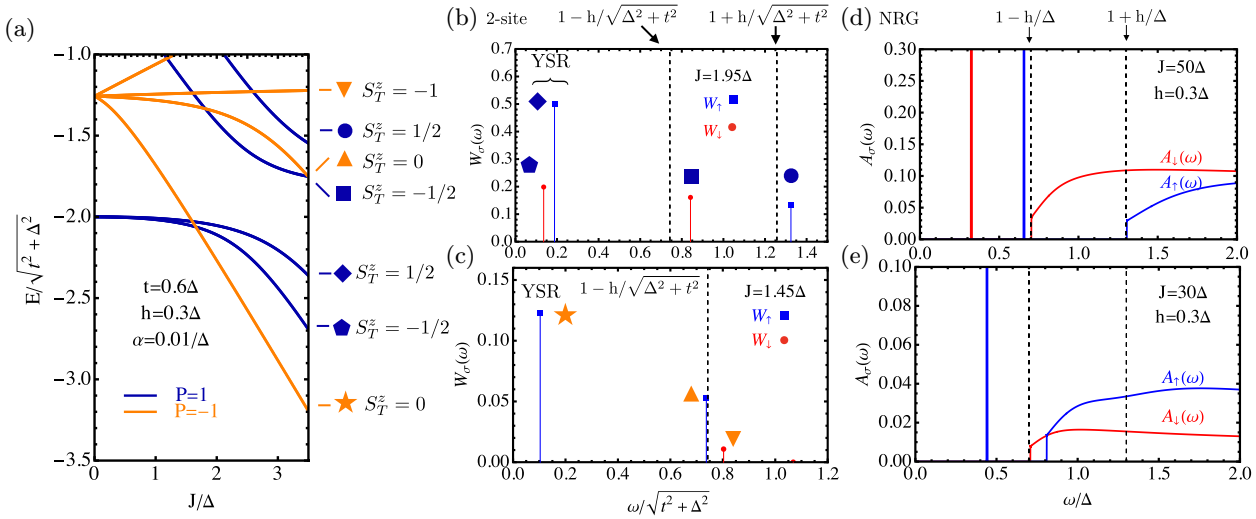

FIG. 4. (a) Low-energy spectrum of the two-site model [cf. Eq. (5)] labeled by the fermion parity $P = \pm 1$ and z component of the total spin S^z_T. (b), (c) The spectral weights in the strong- and weak-coupling regimes, respectively, of the discrete excitation peaks, i.e., $W_\sigma(\omega) = \lim_{\epsilon\to 0}\int_{\omega-\epsilon}^{\omega+\epsilon} d\omega'\, A_\sigma(\omega')$, where $A_\sigma(\omega)$ is the spin-resolved spectral function of the two-site model (see main text for details). (d), (e) Plots of $A_\sigma(\omega)$ for the full model in the strong- and weak-coupling regimes, respectively. The dashed vertical lines indicate the positions of the threshold for continuum excitations in the classical model described in Ref. [61]. Red and blue correspond to spin-up and spin-down components of $A_{\sigma=\{\uparrow,\downarrow\}}(\omega)$, respectively.

Hamiltonian reads

$$\begin{aligned} H &= H_0 + H_K + H_{\mathrm{RKKY}}, \\ H_0 &= \sum_{i=0,1} \left[\Delta(c^\dagger_{i\uparrow} c^\dagger_{i\downarrow} + \mathrm{H.c.}) + h\, c^\dagger_{i\sigma}\left(2s^z_{\sigma\sigma'}\right)c_{i\sigma'}\right] \\ &\quad - t(c^\dagger_{0\sigma} c_{1\sigma} + \mathrm{H.c.}), \\ H_K &= \frac{J}{2}(S^+ s^-_0 + \mathrm{H.c.}) + J S^z s^z_0, \\ H_{\mathrm{RKKY}} &= Jh\alpha S^z. \end{aligned} \tag{5}$$

In the above expression, we have explicitly written the spin-flip and Ising parts of the exchange interaction by introducing $S^\pm = S^x \pm iS^y$, $s^\pm_0 = s^x_0 \pm i s^y_0$, etc. Note that in the two-site model, the spectrum is discrete and therefore there is no Pauli paramagnetism. Thus, we have replaced the density of states at the Fermi energy, ρ_0, with a phenomenological constant α, that parametrizes the strength of the RKKY interaction between the impurity and the FMI.

The Hilbert space of this model has a relatively small dimension ($= 32$) and thus full exact diagonalization of the Hamiltonian (5) is possible. Moreover, the numerical calculations are aided by the existence of a few conserved quantities. The fermion-parity operator takes the form $P = (-1)^{\sum_{i\sigma} n_{i\sigma}}$, where $n_{i\sigma} = c^\dagger_{i\sigma} c_{i\sigma}$ ($i = 0, 1$). The system is also invariant under a global spin rotation around the z axis and, therefore, along with P, $S^z_T = S^z + \sum_{i=0,1} c^\dagger_{i\sigma} s^z_{\sigma\sigma'} c_{i\sigma'}$ is also conserved. Thus, the eigenstates of the Hamiltonian in Eq. (5) can be labeled by their fermion parity: even ($P = +1$) or odd ($P = -1$), and the eigenvalue of S^z_T.

B. Exact-diagonalization results

We demonstrate that the two-site model qualitatively reproduces the key spectral properties found in NRG. We obtain the spectrum of the two-site model by diagonalizing the Hamiltonian in Eq. (5). Figure 4(a) shows the low-energy spectrum of the two-site model as a function of the exchange coupling J. When $J = 0$, the system is in the even-parity twofold (doublet) degenerate ground state with the eigenvalue of S^z_T (S^z) equal to $\pm 1/2$ and the ground-state energy is $E_0 = -2\sqrt{\Delta^2 + t^2}$. In the basis of bonding and antibonding creation (annihilation) operators, $c^{(\dagger)}_{\pm\sigma} = (c^{(\dagger)}_{0\sigma} \pm c^{(\dagger)}_{1\sigma})/\sqrt{2}$, the doublet is $|\mathrm{GS}_m\rangle = |\mathrm{BCS}\rangle_+ |\mathrm{BCS}\rangle_- |m = \pm\tfrac{1}{2}\rangle$, where $|\mathrm{BCS}\rangle_\pm = (u_\pm|0\rangle_\pm + v_\pm|2\rangle_\pm)/\sqrt{2}$ and $c_{\pm\sigma}|0\rangle_\pm = 0$, $|2\rangle_\pm = c^\dagger_{\pm\downarrow} c^\dagger_{\pm\uparrow}|0\rangle$. The expressions of $u_\pm$ and $v_\pm$ in terms of Δ, t, h can be found in Appendix D.

The model has two different ground states, depending on the strength of the exchange coupling J. In the weak-coupling regime ($J < J_{\mathrm{cr}}$), the impurity spin is weakly entangled with the superconducting sites and remains unscreened. The ground state is adiabatically connected with one of the states of the $J = 0$ doublet, which is a product of even-parity states. As J increases, the Kondo singlet, which roughly corresponds to an entangled state of the impurity spin and a quasiparticle localized in the two sites, is gradually pushed down in energy [see Fig. 4(a)]. Eventually, at $J = J_{\mathrm{cr}} \simeq 1.5\Delta$, the system undergoes a level-crossing phase transition, changing the fermion parity of the ground state from even to odd, such that the singlet state eventually becomes the ground state in the strong-coupling limit ($J > J_{\mathrm{cr}}$).

Notice that for $h = 0$, time-reversal symmetry is restored and the (Kramers) degeneracy of the ground state in the weak-coupling limit is guaranteed. In this regime, provided there is no bias in the preparation of the system, the ground state is described by a mixed state with equal (classical) probability for the two states of the doublet [61]. However, setting $h \neq 0$ breaks time-reversal symmetry and lifts the degeneracy of the even-parity ground-state doublet. Thus, as found in the NRG results for the full model (1), in the two-site model for $J < J_{\mathrm{cr}}$, we also observe that the degeneracy of the $h = 0$ doublet is lifted and a finite splitting between the two lowest-lying even-parity states (denoted δE_0 from here on) appears. Notice that $\delta E_0 \neq 0$, even for small J, and it increases with J up to a maximum $\Delta E_0 = 2h$, that is, twice the Zeeman energy caused by the exchange field. Therefore, the behavior of δE_0 qualitatively reproduces the NRG results (compare the two panels of Fig. 3). Furthermore, in the two-site model, as shown below analytically, the splitting is linear in J at vanishing hopping amplitude (i.e., for $t = 0$). In this limit, the two-site model reduces to a single-site model studied in Ref. [61] in an RKKY-like (magnetic) field $\propto J$. This model fails to reproduce the spectral features observed in NRG.

The two-site model offers a rather simple explanation for the saturation of the splitting δE_0 to twice the Zeeman energy at large Kondo coupling, i.e., $\delta E_0(J \to +\infty) \to 2h$ (cf. Fig. 3). This saturation is observed both in NRG and in the two-site model and can be understood as follows: For large J, the impurity captures a quasiparticle and localizes it in the first site of the chain (i.e., the $i = 0$ site). The captured quasiparticle and the impurity form a tightly bound Kondo singlet with binding energy $\sim -\frac{3}{4}J$ for large $J \gg t, \Delta, h$. In this limit, the RKKY interaction acting on the impurity spin alone has zero expectation value, and hopping from the site $i = 1$ into the site $i = 0$, and vice versa, is also suppressed. Thus, the single-particle excitations of the system must "live" on the site(s) with $i > 0$. If we neglect the hopping amplitude t in this large-J limit, the lowest quasiparticle excitations at energy Δ are spin split due to the exchange field by an amount equal to $2h$. Notice that since the (Kondo) singlet ground state has odd fermion parity, the lowest-energy quasiparticle excitations over this ground state have even parity, and therefore $2h$ is the smallest spin splitting of even-parity states for $J \to +\infty$.

V. PERTURBATION THEORY

In what follows, we use perturbation theory to analytically obtain the splitting δE_0 in the weak-coupling regime where $J \ll \Delta, h, t$. In this regime, there are two contributions responsible for the splitting of the lowest-lying even-parity states: the effective RKKY interaction induced by the FMI, which is of the order of $O(J)$ and the different kind of triplet correlations built into the spin-split superconductor, which appears at $O(J^2)$,

$$\delta E_0 = \delta E^{(1)}_0 + \delta E^{(2)}_0, \tag{6}$$

where the term linear in both J and h is given by

$$\delta E_0^{(1)} = \langle \mathrm{GS}_{m=+\frac{1}{2}} | H_{\mathrm{RKKY}} | \mathrm{GS}_{m=+\frac{1}{2}} \rangle \tag{7}$$

$$- \langle \mathrm{GS}_{m=-\frac{1}{2}} | H_{\mathrm{RKKY}} | \mathrm{GS}_{m=-\frac{1}{2}} \rangle. \tag{8}$$

For the calculation of the second-order contribution, the starting point is the following expression of the energy splitting of the lowest-lying even-parity states, whose derivation is discussed in Appendix A:

$$\delta E_0^{(2)} = \frac{J^2}{4}(\chi^{+-} - \chi^{-+}), \tag{9}$$

where

$$\chi^{ab} = -\int_0^{+\infty} d\tau\, C^{ab}(\tau) \tag{10}$$

$$= \sum_E \frac{\langle \mathrm{BCS}|s^a|E\rangle\langle E|s^b|\mathrm{BCS}\rangle}{E - E_0}, \tag{11}$$

$$\mathcal{C}^{ab}(\tau) = -\langle \mathrm{BCS}|\mathcal{T}[s^a(\tau)s^b(0)]|\mathrm{BCS}\rangle. \tag{12}$$

Equation (11) is most useful when dealing with the finite-size system described by Eq. (5). The expression in terms of the time-ordered spin correlation functions $\mathcal{C}^{ab}(\tau)$ will be useful for carrying out the perturbative calculation in the case of an extended (infinite) superconductor. In Eq. (11), $|\mathrm{BCS}\rangle$ and $|E\rangle$ are, respectively, the ground-state and excited states of the superconductor Hamiltonian H_0 [cf. Eqs. (1) and (5)].

A. Two-site model

Let us first consider the two-site model. The first-order-in-J correction to the spitting of the ground-state energy comes from the RKKY term H_{RKKY} in the Hamiltonian (5) and it reads

$$\delta E_0^{(1)} = Jh\alpha. \tag{13}$$

In order to compute χ^{+-} and χ^{-+}, we use

$$s_0^{\pm}|\mathrm{BCS}\rangle = \mp\lambda|t_{\pm 1}\rangle, \tag{14}$$

where λ is a function of t, Δ, h (for details, see Appendix D), $|\mathrm{BCS}\rangle = |\mathrm{BCS}\rangle_+|\mathrm{BCS}\rangle_-$, and we have introduced the spin-triplet quasiparticle states:

$$|t_{+1}\rangle = |\uparrow\uparrow\rangle = \gamma_{+,\uparrow}^\dagger \gamma_{-,\uparrow}^\dagger |\mathrm{BCS}\rangle, \tag{15}$$

$$|t_0\rangle = \frac{(|\uparrow\downarrow\rangle + |\downarrow\uparrow\rangle)}{\sqrt{2}}$$

$$= \frac{1}{\sqrt{2}}[\gamma_{+,\uparrow}^\dagger \gamma_{-,\downarrow}^\dagger + \gamma_{-,\uparrow}^\dagger \gamma_{+,\downarrow}^\dagger]|\mathrm{BCS}\rangle, \tag{16}$$

$$|t_{-1}\rangle = |\downarrow\downarrow\rangle = \gamma_{+,\downarrow}^\dagger \gamma_{-,\downarrow}^\dagger |\mathrm{BCS}\rangle, \tag{17}$$

where $\gamma_{\pm,\sigma}$ ($\gamma_{\pm,\sigma}^\dagger$) destroys (creates) a quasiparticle in the bonding (–) and antibonding (+) orbitals with spin σ. The triplet states have eigenenergies $E = \{E_{t_{+1}}, E_{t_0}, E_{t_{-1}}\} = \{2h, 0, -2h\}$, respectively. The ground-state energy is $E_0 = -2\sqrt{\Delta^2 + t^2}$.

To the lowest order in perturbation theory, the doublet $|\mathrm{GS}_m\rangle = |\mathrm{BCS}\rangle|m = \pm\frac{1}{2}\rangle$ is coupled to spin-triplet quasiparticle excitations via the Kondo exchange H_K. Since the energy of $|t_{\pm 1}\rangle$ is split by the exchange field, this results in the following splitting of the lowest-energy even-parity states:

$$\delta E_0^{(2)} = \frac{J^2 t^2 h}{16(t^2 + \Delta^2)(\Delta^2 - h^2 + t^2)}, \tag{18}$$

$$\simeq \frac{J^2 t^2 h}{16(t^2 + \Delta^2)^2} + O(h^3), \tag{19}$$

to the leading order in J and h. Notice that the splitting in Eq. (18) vanishes either in the absence of exchange field $h = 0$ or for $t = 0$, which is the limit of a single-site model, in agreement with the previous findings in Ref. [61].

To summarize, in the weak-coupling limit, the two-site model shows the splitting of the two lowest-lying even-parity states. In this model, the contribution of $O(J^2)$ to the splitting originates from the coupling of the doublet states at $J = 0$ to the spin-split triplet states containing two quasiparticles. This result also clarifies why the single-site model of Ref. [61] does not describe this second-order contribution to the splitting $\delta E_0^{(2)}$. Indeed, the minimum number of independent orbitals required to construct a spin-triplet with two quasiparticles is two (the bonding and antibonding orbitals $\pm$ for the two-site model).

B. Extended superconductor

In the case of the extended superconductor, the first-order contribution to the splitting is determined by the expectation value of H_{RKKY} according to Eq. (7). This yields

$$\delta E_0^{(1)} = Jh\rho_0. \tag{20}$$

Concerning the contribution of $O(J^2)$, starting from Eq. (9), this contribution can be written in terms of singlet and triplet components of the local single-particle Green's function $\mathcal{G}^0(i\omega)$ as follows:

$$\delta E_0^{(2)} = \frac{J^2}{4}\int \frac{d\omega d\omega'}{2\pi} \frac{\mathrm{Tr}[g_s(i\omega)g_t(i\omega - i\omega')]}{i\omega}, \tag{21}$$

where the 2×2 Nambu matrices $g_s(i\omega)$ and $g_t(i\omega)$ are the singlet and triplet components of $\mathcal{G}^0(i\omega)$ [see Eqs. (B4) and (B5) in Appendix B for explicit expressions]. Since the triplet component $g_t(i\omega) \to 0$ for $h \to 0$, the above result clearly shows that $\delta E_0^{(2)}$ vanishes in the absence of the triplet correlations. Interestingly, in the opposite strong-coupling regime, where the above perturbative treatment does not apply, the triplet correlations encoded in g_t are also responsible for the splitting of the quasiparticle bands, which results in $\delta E_0 \to 2h$. This intuition is confirmed by the NRG analysis for the extended model and the exact-diagonalization results for the two-site model shown in Fig. 3: The energies of the two lowest-lying even-parity states evolve smoothly from the weak- to the strong-coupling regime. This is also important from the experimental point of view because, in the tunneling spectrum, the splitting can only be observed in the strong-coupling regime; see center and right panels of Fig. 4.

The expression in Eq. (21) can be evaluated explicitly and in the wide band limit, with logarithmic accuracy, it takes the form

$$\delta E_0^{(2)} \simeq (J\rho_0)^2 h \ln\left(\frac{D}{\Delta}\right), \tag{22}$$

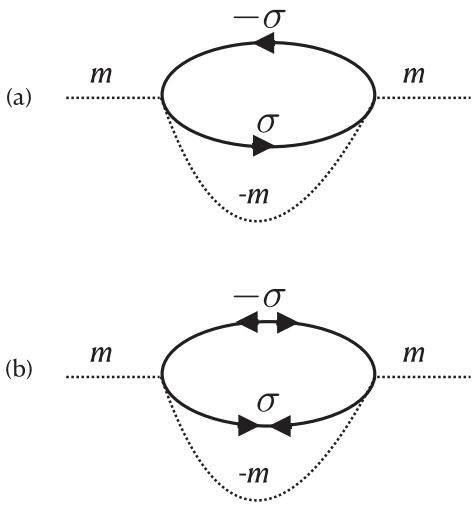

FIG. 5. (a) Normal and (b) anomalous Feynman diagrams contributing in second-order perturbation theory to the energy splitting of the two lowest-lying eigenstates with even fermion parity. The energy splitting is the difference between the $m = +\frac{1}{2}$ and $m = -\frac{1}{2}$ diagrams. The dashed lines describe the impurity state and the continuous lines correspond to the superconductor. The normal contribution (a) is logarithmically divergent. See Appendices A and C for details.

where D ($\sim\omega_D$ in conventional superconductors) is the bandwidth of the superconductor described by H_0 term in Eq. (1) (see Appendix C for details). Thus, combining the two contributions, we find the ratio of the splitting to the exchange field h to be

$$\delta E_0/h = J\rho_0 + (J\rho_0)^2 \ln\left(\frac{D}{\Delta}\right) + O(J^3). \tag{23}$$

Figure 2 shows that this behavior reproduces the splitting in the regime of small J observed in the NRG results. However, the prefactor in the second-order term predicted by the above perturbative treatment is different because the NRG implements a different (lattice) regularization of the impurity Hamiltonian. In other words, the presence of a logarithm is a clear indication that the perturbative expression for $\delta E_0^{(2)}/h$ is not universal in the weak-coupling limit. In the case of the two-site model, the lack of universality of the perturbative result is manifested in that $\delta E_0^{(2)}/h \propto t$, where $t \sim D$ is a hopping amplitude between the two superconducting sites. Indeed, closer examination reveals that the logarithmic correction in Eqs. (22) and (23) arises from the noncommutative spin-flip scattering processes that appear in the perturbation theory of the Kondo Hamiltonian and, specifically, from the normal contribution whose Feynman diagram is depicted in Fig. 5(a). Indeed, using renormalized perturbation theory, we could have anticipated the appearance of the logarithm. Let us begin by assuming $\rho_0 J \to 0$, so that the energy splitting is well approximated by the first-order result $\delta E_0 = \rho_0 J h$. Under renormalization, the exchange coupling constant $g(D) = \rho_0 J(D)$ flows according to [64]

$$\bar{D}\frac{dg(\bar{D})}{d\bar{D}} = -g^2(\bar{D}). \tag{24}$$

This equation can be integrated from the scale of the initial bandwidth $D \sim \omega_D$ down to the scale of the gap Δ, where the renormalization stops. This yields

$$\begin{aligned}\rho_0 J(\Delta) &= \frac{1}{[\rho_0 J]^{-1} - \ln(D/\Delta)} \\ &= \rho_0 J + (\rho_0 J)^2 \ln\frac{D}{\Delta} + \cdots,\end{aligned} \tag{25}$$

where $J = J(D)$ is the *bare* Kondo coupling at the scale of $D \sim \omega_D$. Provided the coupling remains small, i.e., $\rho_0 J(\Delta) \ll 1$, it is still possible to approximate $\delta E_0/h$ by the first-order perturbative result, i.e., $\delta E_0/h = \rho_0 J(\Delta)$. Rewriting $\rho_0 J(\Delta)$ in terms of the bare coupling $\rho_0 J$, we find an infinite series of logarithmic corrections. Furthermore, using this approach, we can also remove the unpleasant dependence of δE_0 on the nonmeasurable quantities D and J by replacing them with a much more physical energy scale, namely, the scale at which the renormalized coupling $g(\bar{D}) = \rho_0 J(\bar{D})$ diverges and defines the Kondo temperature, $T_K = D\exp[-1/(\rho_0 J)]$ [64]. Inserting T_K into Eq. (25), we obtain

$$\rho_0 J(\Delta) = \frac{1}{\ln\left(\frac{\Delta}{T_K}\right)}, \tag{26}$$

and, therefore, provided $T_K \ll \Delta$ (i.e., the weak-coupling regime),

$$\delta E_0/h = \rho_0 J(\Delta) = \frac{1}{\ln\left(\frac{\Delta}{T_K}\right)}. \tag{27}$$

In the opposite limit, the strong-coupling regime where $T_K \gg \Delta$, NRG yields $\delta E_0/h \to 2$, independent of T_K/Δ. It is possible to interpolate between the two regimes by writing the ratio $\delta E_0/h$ as a single-parameter scaling function of T_K/Δ, i.e.,

$$\delta E_0 = F\left(\frac{T_K}{\Delta}\right), \tag{28}$$

where $F(x) \simeq (-\ln x)^{-1}$ for $x \ll 1$ and $F(x) \to 2$ for $x \to +\infty$. The shape of this scaling function, as obtained when plotting the NRG data for $\delta E_0/h$ as a function of T_K/Δ, is shown in Fig. 6.

Finally, let us emphasize that none of these features are captured by the classical treatment [50–52,61]. Indeed, as we shall describe below, there are also other features of the NRG results that are not captured by the classical treatment.

VI. OTHER SPECTRAL FEATURES

Next, we turn our attention to describing the effect of the exchange field of the FMI on the quasiparticle continuum which may be observed in the tunneling spectra. Indeed, NRG shows that other interesting features concern the continuum threshold of single-particle excitations; see Figs. 4(d) and 4(e). To understand the origin of these features, it is worth recalling the expression of the spectral function at positive energies and zero temperature,

$$A_\sigma(\epsilon > 0) = \sum_\alpha |\langle\Phi_\alpha|O_\sigma^\dagger|\Phi_0\rangle|^2 \delta(\epsilon + E_\alpha - E_0), \tag{29}$$

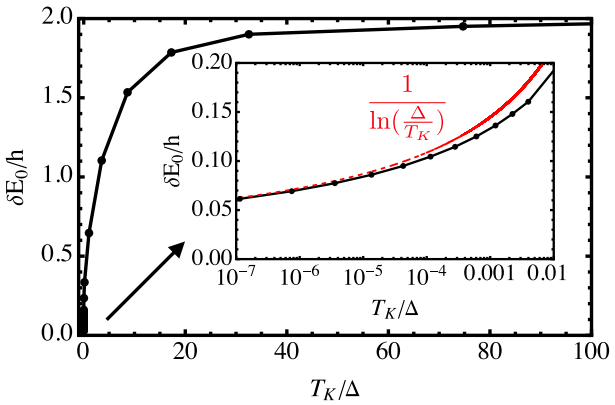

FIG. 6. Ratio of the energy splitting of the two lowest even-parity states δE_0 to the exchange field of the ferromagnetic insulator h vs the ratio of the Kondo temperature T_K to the superconducting gap Δ. The Kondo temperature is extracted from the half width at half maximum [65] of the Kondo peak computed from NRG for a spin-$\frac{1}{2}$ impurity with Kondo coupling J to a normal metal. For $T_K/\Delta \ll 1$, the splitting behaves as $1/\ln(\Delta/T_K)$ and saturates to 2 for $T_K/\Delta \gg 1$.

where $|\Phi_0\rangle$ is the ground state and $|\Phi_\alpha\rangle$ the excited state of the system. We have introduced the operators $O_\sigma^\dagger = [H_K, c_{0\sigma}^\dagger]$, where $c_{0\sigma}^\dagger = \sum_{\boldsymbol{k}} c_{\boldsymbol{k}\sigma}^\dagger/\sqrt{\Omega}$ creates a fermion with spin σ at the position of the impurity. Evaluating the expressions for $O_\sigma^\dagger$ explicitly, we find

$$O_\uparrow^\dagger = \frac{J}{2}(S^+ c_{0,\downarrow}^\dagger + S^z c_{0\uparrow}^\dagger), \tag{30}$$

$$O_\downarrow^\dagger = \frac{J}{2}(S^- c_{0,\uparrow}^\dagger - S^z c_{0\downarrow}^\dagger). \tag{31}$$

When the spin is treated as a classical vector, i.e., Refs. [50–52], the terms proportional to $S^\pm$ are neglected and the above operators are approximated as $O_\sigma \approx \pm S^z c_{0\sigma}$ (where $+$ is for $\sigma = \uparrow$ and $-$ for $\sigma = \downarrow$) [66]. Thus, $A_\sigma(\epsilon)$ reduces to the imaginary part of the Fourier transform of the local (retarded) Green's function, $G_\sigma^R(t) = -i\theta(t)\langle\{c_{0\sigma}(t), c_{0\sigma}^\dagger(0)\}\rangle$. The calculation of the spectral function for a magnetic impurity coupled to a spin-split superconductor in the classical approximation was reported in Ref. [61]. It yields spin-dependent threshold energies, $\epsilon_{B\sigma} = \Delta \pm h$, for the continuum of single-particle excitations, which does not differ from the one obtained from the unperturbed Green's functions of the superconductor [cf. (B5) in Appendix B], independently of whether the impurity is in the strong- or weak-coupling regime.

On the other hand, NRG yields a very different picture; see Figs. 4(d) and 4(e). In the strong-coupling limit, the value of the threshold energy is $\epsilon_{B\sigma} = \Delta \pm h$ and agrees with the result obtained from the classical approximation. However, in the weak-coupling limit, where the classical approximation is expected to be more accurate, NRG shows that $\epsilon_{B\uparrow}$ undergoes a downward shift from its "classical" value $\Delta + h$ and becomes almost equal to $\epsilon_{B\downarrow} \simeq \Delta - h$ [see Fig. 4(d)]. To better understand the origin of this shift in $\epsilon_{B\uparrow}$, let us first recall that for $h > 0$, the ground state in the weak-coupling regime is an eigenstate of S_T^z with eigenvalue $m = -\frac{1}{2}$, i.e., $S_T^z|\Phi_0\rangle = (-\frac{1}{2})|\Phi_0\rangle$. As pointed out above, this state is, to a large extent, well approximated by the product state $|\mathrm{BCS}\rangle|-\frac{1}{2}\rangle$. Mathematically, this is expressed by the following equation:

$$|\Phi_0\rangle = Z^{1/2}|\mathrm{BCS}\rangle\big|-\tfrac{1}{2}\big\rangle + \cdots, \tag{32}$$

where $Z \lesssim 1$ and the ellipsis stays for other components of the state containing, e.g., quasiparticle triplet excitations similar to those discussed in Sec. V A for the two-site model. Using this insight, we notice that for $h > 0$, the action of the operators $O_\sigma^\dagger$ on the ground state produces quite different results,

$$O_\uparrow^\dagger|\Phi_0\rangle = \frac{J}{2}\big(Z^{1/2}c_{0\downarrow}^\dagger|\mathrm{BCS}\rangle\big|+\tfrac{1}{2}\big\rangle - \frac{1}{2}Z^{1/2}c_{0\uparrow}^\dagger|\mathrm{BCS}\rangle\big|-\tfrac{1}{2}\big\rangle\big) + \cdots, \tag{33}$$

$$O_\downarrow^\dagger|\Phi_0\rangle = \frac{J}{2}Z^{1/2}c_{0\downarrow}^\dagger|\mathrm{BCS}\rangle\big|-\tfrac{1}{2}\big\rangle + \cdots. \tag{34}$$

Equation (33) shows that when an electron with spin antialigned with the ground-state projection of S_T^z tunnels, it can flip in the impurity spin. However, no such spin flip is produced when the spin is aligned with the S_T^z projection of the weak-coupling ground state. The spin flip has important consequences for the single-particle excitations created in the superconductor by $c_{0\downarrow}$: By flipping the spin of the impurity from $|-\frac{1}{2}\rangle$ to $|+\frac{1}{2}\rangle$, the Ising term of H_K, that is, $JS^z s_0^z$, changes from repulsive to attractive for single-particle excitations with $\sigma = \downarrow$. In other words, some of the excitations created by $S^+ c_{0\downarrow}^\dagger$ live in a sector of the Hilbert space where the Ising term has the opposite sign to those excitations created by $S^z c_{0\uparrow}^\dagger$. The attractive character of the Ising term induces an "excitoniclike" [67] shift of the excitation energies and therefore the threshold energy for the continuum $\epsilon_{B\uparrow}$ becomes lower than the classical value $\Delta + h$. Let us point out that for $h = 0$, no such shift occurs because the ground state is a degenerate doublet and the spectral function must be averaged over the two states of the doublet [61]. Thus, the spin-flip contribution is equal to zero by time-reversal symmetry. Similarly, for $h \neq 0$ in the strong-coupling regime, the ground state is a singlet and therefore contains components of both spin orientations of the impurity, which are strongly entangled with a cloud of quasiparticle excitations in the superconductor. Since the spin projection of the impurity rapidly fluctuates in a singlet, the Ising term of H_K should not affect the energy of single-particle excitations.

Finally, let us point out that the effects described above are also qualitatively captured by the two-site model introduced in Sec. IV. For this model, we can also compute the spectral function using the same operators O_σ as in the NRG case. For $J < J_{\mathrm{cr}}$, we find that the spin-down component of the continuum part of the spectral function shifts by $-h - \delta h$, while the spin-up component shifts by a different amount of $-h$. Figures 4(b) and 4(c) show this different behavior of the spin-up and spin-down components of the spectral function in the weak- and strong-coupling regimes of J.

VII. CONCLUSIONS

We have investigated a system of a single magnetic impurity on the surface of a ferromagnetic insulator (FMI)/superconductor (SC) heterostructure, where the SC has a thickness smaller than the coherence length. Under such conditions, the proximity effect of the FMI on the SC and impurity is twofold: First, it splits the energy of the Bogoliubov quasiparticle states without destroying the superconducting state. Second, it leads to a spin polarization of the surface of the superconductor that contains the impurity, which results in an RKKY-like interaction between the latter and the FMI. We have studied this system by applying the numerical renormalization group method (NRG).

From the NRG calculations, we obtained the ground-state and low-energy excitations of the system as a function of the (Kondo) exchange of the impurity. The latter drives a quantum phase transition from a unique even-parity ground state to a (unique) singlet ground state. Our main result is the energy splitting of the even-parity doublet with total spin $\pm\frac{1}{2}$ induced by the magnetic proximity effect. The splitting already occurs in the regime of weak exchange coupling J and grows smoothly with J saturating in the strong-coupling limit to twice the value of the exchange field with the FMI. In the strong-coupling regime, the splitting is observable in the spectra acquired using the scanning tunneling microscope as the splitting of the YSR excitations.

In the limit of weak Kondo coupling J, we have computed the splitting using perturbation theory. The splitting contains a first-order correction in J from the RKKY-like interaction and a second-order correction from the noncommutative Kondo-like scattering with the host electrons. The second-order correction has the form of a typical Kondo logarithm, which is cut off by the superconducting gap Δ. This result has also been rederived using scaling, and when combined with the numerical observation of the saturation at large J, it allows us to conjecture that the ratio of the splitting to the FMI exchange field can be written as a single-parameter scaling function of T_K/Δ, where T_K is the Kondo temperature of the impurity. Additionally, we have also discussed the shift of the threshold for the continuum of single-particle excitations observed in the spin-resolved spectral function computed using NRG. The shift occurs in the weak-coupling regime only for tunneling electrons with the spin opposite to the spin of the impurity in the ground state and has been qualitatively explained as an excitoniclike effect. Together with the splitting of the even-parity ground-state doublet, this effect cannot be captured by the classical approach of Yu, Shiba, and Rusinov [50–52] when generalized to the quantum impurity model in Ref. [61].

For a qualitative understanding of the underlying physics of this system, we have employed a two-site model, where the superconductor is represented by two spinful fermion sites with the impurity spin coupled to one of them. This minimal model correctly captures the behavior of energy splitting of the even-parity doublet and provides an intuitive picture in terms of coupling to triplet excitations to explain the physics behind it. It also qualitatively explains the shift of the threshold referred to above.

The splitting is proportional to the exchange field of the FMI and it can be quite sizable for a sufficiently large Kondo coupling. It therefore allows using the FMI to control the spin of the impurity and its excitations *in the absence* of an external magnetic field. This happens even though the FMI is located rather far (typically tens of nm) from the impurity. It was already pointed out in Ref. [61] that the exchange field of the FMI leads to robust spin polarization of the YSR states. This effect is further enhanced by the magnetic and triplet correlations discussed in this work. Besides the STM in the strong-coupling regime, where the splitting of the doublet is observable as the splitting of the YSR peaks for the two spin orientations, the splitting may also be observable by measuring the microwave absorption of a dilute ensemble of impurities on the surface of the FMI/SC.

ACKNOWLEDGMENTS

M.A.C. and S.B. thank Ilya Tokatly for useful discussions on the magnetic proximity effect. This work has been supported by the Agencia Estatal de Investigación del Ministerio de Ciencia e Innovación (Spain) (MCIN/AEI) through Grants No. PID2020-120614GB-I00/AEI/10.13039/501100011033 (ENACT), No. PID2020-114252GB-I00/AEI/10.13039/501100011033, and No. TED2021-130292B-C42. C.-H.H. acknowledges support from a Ph.D. fellowship from DIPC. A.S. acknowledges funding from the Basque Government's IKUR Initiative on Quantum Technologies (Department of Education). F.S.B. has received funding from the European Union's Horizon Europe research and innovation programme under Grant Agreement No. 101130224 (JOSEPHINE).

APPENDIX A: SPIN SPLITTING IN PERTURBATION THEORY

The Hamiltonian describing a magnetic impurity in the spin-split superconductor has been introduced in Sec. II. In this Appendix, to make the notation more compact, we shall rewrite it as follows:

$$H = H_0 + H_I, \tag{A1}$$

$$H_I = J\boldsymbol{S}\cdot\boldsymbol{s}_0 + J\rho_0 h S^z, \tag{A2}$$

where H_0 describes the clean spin-split superconductor [cf. Eq. (2)] and $H_I = H_K + H_{\mathrm{RKKY}}$ describes all the interactions of the impurity with its host; $\boldsymbol{s}_0$ is the spin-density operator of the superconductor at the location of the impurity; $\boldsymbol{S}$ is the impurity spin operator.

Let us compute the free energy in perturbation theory. We start with the following perturbation theory result for the shift of the grand-canonical free energy at absolute temperature T,

$$\begin{aligned}\Delta F^m &= F^m - F_0 \\ &= -T\ln\left\{\langle m|\left\langle \mathcal{T}\exp\left[-\int_0^{1/T} d\tau\, H_I(\tau)\right]\right\rangle|m\rangle\right\} \\ &= T\int_0^{1/T} d\tau_1\, \langle m|\langle H_I(\tau_1)\rangle|m\rangle\end{aligned}$$

$$-\frac{T}{2}\int_0^{1/T} d\tau_1 d\tau_2\, \langle m|\langle \mathcal{T}[H_I(\tau_1)H_K(\tau_2)]\rangle|m\rangle + O(J^3). \tag{A3}$$

In the above expression, $\langle\cdot\rangle$ stands for the average over the canonical ensemble of the eigenstates of the superconductor Hamiltonian H_0 and $|m=\pm\frac{1}{2}\rangle$ are the eigenstates of decoupled magnetic impurity with $S^z=\pm\frac{1}{2}$. In this basis, the first-order term vanishes because $\langle s_0\rangle = 0$. Note that we do not allow the state of the impurity to fluctuate thermally because we are interested in computing the ground-state energy difference between the $m=+\frac{1}{2}$ and $m=-\frac{1}{2}$ configurations. Since the unperturbed ground state is the product state of the BCS wave function and a single impurity spin, the first-order contribution of H_K vanishes. The first-order term is simply given by the RKKY contribution,

$$\Delta F^{(1,m)} = J\rho_0 h m, \tag{A4}$$

that leads to the splitting in energy,

$$\Delta E_0^{(1)} = J\rho_0 h. \tag{A5}$$

Introducing Eq. (A2), we obtain the second-order contribution,

$$\Delta F^{(2,m)} = -\frac{J^2T}{2}\int_0^{1/T} d\tau_1 d\tau_2 \langle m|\mathcal{T}[S^a(\tau_1)S^b(\tau_2)]|m\rangle \times \left\langle \mathcal{T}\left\{\left[\rho_0 h\delta_{a,z}+s_0^a(\tau_1)\right]\left[\rho_0 h\delta_{b,z}+s_0^b(\tau_2)\right]\right\}\right\rangle + O(J^3). \tag{A6}$$

Next, we compute the impurity-spin correlation function. Assuming $\boldsymbol{S}$ to be a spin-$\frac{1}{2}$ operator, we have

$$\begin{aligned}&\langle m|\mathcal{T}[S^a(\tau_1)S^b(\tau_2)]|m\rangle\\ &= \theta(\tau_1-\tau_2)\langle m|S^aS^b|m\rangle + \theta(\tau_2-\tau_1)\langle m|S^bS^a|m\rangle\\ &= \frac{1}{4}\delta^{ab} + \frac{i}{2}\epsilon^{abc}\langle m|S^c|m\rangle \times \mathrm{sgn}(\tau_1-\tau_2),\end{aligned}$$

where we used the Pauli-matrix identity $S^aS^b = \frac{1}{4}\delta^{ab}\mathbb{I} + \frac{i}{2}\epsilon^{abc}S^c$. Note that $\langle m|S^c|m\rangle = \delta^{z,c}m$ because S^z is the only diagonal spin operator in the basis $|m\rangle$. Hence, since, we are interested only in the difference between $\Delta F^{(2,m=+\frac{1}{2})}$ and $\Delta F^{(2,m=-\frac{1}{2})}$, the splitting of the free energy is given by

$$\Delta F_0^{(2)} = \Delta F^{(2,m=+\frac{1}{2})} - \Delta F^{(2,m=-\frac{1}{2})} \simeq \frac{iJ^2T}{4}\int_0^{1/T} d\tau_1 d\tau_2\, \mathcal{C}^z(\tau_1-\tau_2)\mathrm{sgn}(\tau_1-\tau_2). \tag{A7}$$

In the last line, we have introduced the correlation function

$$\mathcal{C}^z(\tau) = \epsilon^{ab,z}\mathcal{C}^{ab}(\tau_1-\tau_2), \tag{A8}$$

$$\mathcal{C}^{ab}(\tau_1-\tau_2) = -\left\langle \mathcal{T}\left[s_0^a(\tau_1)s_0^b(\tau_2)\right]\right\rangle. \tag{A9}$$

Next, let us introduce the Fourier transform of the above spin correlation function,

$$\mathcal{C}^{ab}(\tau_1-\tau_2) = T\sum_{\omega_n} e^{-i\omega_n(\tau_1-\tau_2)}\mathcal{C}^{ab}(i\omega_n), \tag{A10}$$

which yields

$$\Delta F_0^{(2)} = \frac{J^2T}{2}\sum_{\omega_n}\frac{\mathcal{C}^z(i\omega_n)}{\omega_n}. \tag{A11}$$

In the last line, we have used that ($\omega_n = 2\pi nT$)

$$\int_0^{1/T} d\tau_1 d\tau_2\, \mathrm{sgn}(\tau_1-\tau_2)e^{-i\omega_n(\tau_1-\tau_2)} = -\frac{2i}{T\omega_n}. \tag{A12}$$

In addition, using $S^\pm = S^x \pm iS^y$, we have

$$\mathcal{C}^z(\omega_n) = \frac{i}{2}[\mathcal{C}^{+-}(i\omega_n) - \mathcal{C}^{-+}(\omega_n)], \tag{A13}$$

where we have used that $\mathcal{C}^{++}(\omega_n) = \mathcal{C}^{--}(\omega_n) = 0$ because of conservation of the total spin z projection, i.e., S_T^z. Therefore,

$$\Delta F_0^{(2)} = \frac{iJ^2T}{4}\sum_{\omega_n}\frac{\mathcal{C}_0^{+-}(i\omega_n) - \mathcal{C}_0^{-+}(i\omega_n)}{\omega_n} + O(J^3). \tag{A14}$$

Taking the $T\to 0$ limit, the above sum becomes an integral, which equals the ground energy splitting,

$$\delta E_0^{(2)} = -\frac{J^2}{4}\int\frac{d\omega}{2\pi}\left[\frac{\mathcal{C}^{+-}(i\omega) - \mathcal{C}^{-+}(i\omega)}{i\omega}\right] + O(J^3). \tag{A15}$$

Finally, recalling that at $T=0$,

$$\int_0^{+\infty} d\tau\, \mathcal{C}^{ab}(\tau) = \int\frac{d\omega}{2\pi}\frac{\mathcal{C}^{ab}(\omega)}{i\omega}, \tag{A16}$$

we arrive at

$$\delta E_0^{(2)} = -\frac{J^2}{4}\int_0^{+\infty} d\tau[\mathcal{C}^{+-}(\tau) - \mathcal{C}^{-+}(\tau)] + O(J^3). \tag{A17}$$

Indeed, using the spectral representation of the spin correlation functions $\mathcal{C}^{ab}(\tau)$ at $T=0$, i.e.,

$$\begin{aligned}\chi^{ab} &= -\int_0^{+\infty} d\tau\, \mathcal{C}^{ab}(\tau)\\ &= \int_0^{+\infty} d\tau\, \left\langle \mathcal{T}\left[s_0^a(\tau)s_0^b(0)\right]\right\rangle\\ &= \sum_E \frac{\langle \mathrm{BCS}|s_0^a|E\rangle\langle E|s_0^b|\mathrm{BCS}\rangle}{E-E_0},\end{aligned} \tag{A18}$$

we can rewrite Eq. (A17) as the difference,

$$\Delta E_0^{(2)} = \frac{J^2}{4}[\chi^{+-} - \chi^{-+}]. \tag{A19}$$

Indeed, a quicker way to arrive at this expression is to start from the second-order perturbation theory formula

at $T = 0$,

$$\Delta E^{(2)}_{m=1/2} = \sum_{E,n=\pm\frac{1}{2}} \frac{|\langle n|\langle E|H_K|\mathrm{BCS}\rangle|m=+1/2|^2}{E_0 - E}$$

$$= -J^2 \sum_E \left[\frac{1}{4} \frac{\langle \mathrm{BCS}|s^-|E\rangle\langle E|s^+|\mathrm{BCS}\rangle}{E - E_0} \sum_{n=\pm\frac{1}{2}} \left\langle m=+\frac{1}{2}\middle|S^+|n\rangle\langle n|S^-\middle|m=+\frac{1}{2}\right\rangle \right]$$

$$- J^2 \sum_E \left[\frac{\langle \mathrm{BCS}|s^z|E\rangle\langle E|s^z|\mathrm{BCS}\rangle}{E - E_0} \sum_{n=\pm\frac{1}{2}} \left\langle m=+\frac{1}{2}\middle|S^z n\rangle\langle n|S^z\middle|m=+\frac{1}{2}\right\rangle \right] \tag{A20}$$

$$= -J^2 \sum_E \left[\frac{1}{4} \frac{\langle \mathrm{BCS}|s^-|E\rangle\langle E|s^+|\mathrm{BCS}\rangle}{E - E_0} \left\langle m=+\frac{1}{2}\middle|S^+S^-\middle|m=+\frac{1}{2}\right\rangle \right]$$

$$- J^2 \sum_E \left[\frac{\langle \mathrm{BCS}|s^z|E\rangle\langle E|s^z|\mathrm{BCS}\rangle}{E - E_0} \left\langle m=+\frac{1}{2}\middle|(S^z)^2\middle|m=+\frac{1}{2}\right\rangle \right]. \tag{A21}$$

The last term involving $(S^z)^2$ is the same for the other ground state of the doublet with $m = -\frac{1}{2}$ and does not contribute to the splitting. Therefore,

$$\Delta E^{(2)}_0 = -\frac{J^2}{4} \sum_E \left[\frac{\langle \mathrm{BCS}|s^-|E\rangle\langle E|s^+|\mathrm{BCS}\rangle}{E - E_0} \left\langle m=+\frac{1}{2}\middle|S^+S^-\middle|m=+\frac{1}{2}\right\rangle \right]$$

$$+ \frac{J^2}{4} \sum_E \left[\frac{\langle \mathrm{BCS}|s^+|E\rangle\langle E|s^-|\mathrm{BCS}\rangle}{E - E_0} \left\langle m=-\frac{1}{2}\middle|S^-S^+\middle|m=-\frac{1}{2}\right\rangle \right] \tag{A22}$$

$$= \frac{J^2}{4}(\chi^{+-} - \chi^{-+}), \tag{A23}$$

where we have used that $\langle m = -\frac{1}{2}|S^-S^+|m = -\frac{1}{2}\rangle = 1$, etc.

APPENDIX B: DEPENDENCE ON TRIPLET CORRELATIONS

In this Appendix, we evaluate the energy splitting as given by Eq. (A15) by computing the correlation functions $C^{+-}(i\omega)$ and $C^{-+}(i\omega)$. To this end, we recall that in terms of the (four-component) Nambu spinor,

$$\Psi_0 = \begin{pmatrix} c_{0\uparrow} \\ c_{0\downarrow} \\ -c^\dagger_{0\downarrow} \\ c^\dagger_{0\uparrow} \end{pmatrix} = \begin{pmatrix} C_0 \\ C^\dagger_0 i\sigma^2 \end{pmatrix}, \tag{B1}$$

the local spin operator reads $\boldsymbol{s}_0 = \frac{1}{2}\Psi^\dagger_0 \boldsymbol{s}\tau^0\Psi_0$. Thus, using this notation, we can write the correlation functions of interest as follows:

$$\mathcal{C}^{ab}(\tau) = -\langle \mathcal{T}[s^a(\tau)s^b(0)]\rangle$$

$$= \tfrac{1}{2}\mathrm{Tr}[\mathcal{G}^0(-\tau)s^a\tau_0\mathcal{G}^0(\tau)s^b\tau^0]. \tag{B2}$$

To obtain the expression in the last line, we have employed Wick's theorem and rewritten $\mathcal{C}^{ab}(\tau)$ in terms of the fermion local Green's function $\mathcal{G}^0(\tau)$ (see further below for the explicit expression of the latter). Next, upon performing the Fourier transform at $T = 0$, we arrive at

$$\mathcal{C}^{ab}(\omega) = \int d\tau\, e^{i\omega\tau}\mathcal{C}^{ab}(\tau)$$

$$= \frac{1}{2}\int \frac{d\omega'}{2\pi}\mathrm{Tr}[\mathcal{G}^0(i\omega')s^a\tau_0\mathcal{G}^0(i\omega - i\omega')s^b\tau^0]. \tag{B3}$$

In the last line, we have relabeled ω_1 as ω'.

It is convenient to write the local Green's function as follows:

$$\mathcal{G}^0(i\omega) = g^0_s(i\omega)s^0 + g^0_t(i\omega)s^z,$$
$$g^0_s(i\omega) = \tfrac{1}{2}[\mathcal{G}^0_+(i\omega) + \mathcal{G}^0_-(i\omega)], \tag{B4}$$
$$g^0_t(i\omega) = [\mathcal{G}^0_+(i\omega) - \mathcal{G}^0_-(i\omega)],$$

where (in the wide band limit)

$$\mathcal{G}^0_\pm(i\omega) = -\pi\rho_0 \frac{(i\omega \mp h)\tau^0 + \Delta\tau^x}{\sqrt{\Delta^2 - (i\omega \mp h)^2}}. \tag{B5}$$

Hence,

$$\mathcal{C}^{ab}(i\omega) = \tfrac{1}{2}\{\mathrm{Tr}[(g_s \star g_s - g_t \star g_t)(i\omega) \otimes s^a s^b]$$
$$+ \mathrm{Tr}[(g_t \star g_s - g_s \star g_t)(i\omega) \otimes s^z s^a s^b]\}. \tag{B6}$$

In the above expression, we have used the notation

$$(f \star g)(i\omega) = \int \frac{d\omega'}{2\pi} f(i\omega')g(i\omega - i\omega') \tag{B7}$$

for the convolution of two functions $f(i\omega)$ and $g(i\omega)$ of the Matsubara frequency $i\omega$; $\otimes$ stands for the Kronecker product of the matrices in the (particle-hole) Nambu and spin indices. The energy shift is determined by the difference,

$$\mathcal{C}^{+-}(i\omega) - C^{-+}(i\omega) = \tfrac{1}{2}\mathrm{Tr}(g_t \star g_s - g_s \star g_t)(i\omega). \quad \text{(B8)}$$

In the last line, we have used that $\mathrm{Tr}[m \otimes s^z] = 0$ and $\mathrm{Tr}[m \otimes s^0] = 2\,\mathrm{Tr}\,(m)$ for any 2×2 matrices in Nambu indices. Notice that g_s and g_t are 2×2 matrices in the (particle-hole) Nambu indices. We have also used that $s^a, s^b \in \{s^+, s^-\}$ and therefore anticommute with s^z. Hence,

$$\begin{aligned}\chi^{+-} - \chi^{-+} &= -\int \frac{d\omega}{2\pi}\frac{\mathcal{C}^{+-}(i\omega) - \mathcal{C}^{-+}(i\omega)}{i\omega} \\ &= \frac{1}{2}\int \frac{d\omega}{2\pi}\frac{\mathrm{Tr}[g_s \star g_t - g_t \star g_s](i\omega)}{i\omega} \\ &= \int \frac{d\omega}{2\pi}\frac{\mathrm{Tr}[g_s \star g_t](i\omega)}{i\omega}. \end{aligned} \quad \text{(B9)}$$

In the last line, we have used the identity

$$\begin{aligned}\mathrm{Tr}[f \star g](i\omega) &= \int \frac{d\omega'}{2\pi}\mathrm{Tr}\, f(i\omega')g(i\omega - i\omega') \quad \text{(B10)} \\ &= \int \frac{d\omega''}{2\pi}\mathrm{Tr} f(i\omega'' + i\omega)g(i\omega'') \\ &= \int \frac{d\omega''}{2\pi}\mathrm{Tr}\, g(i\omega'')f(i\omega'' + i\omega) \\ &= \mathrm{Tr}[g \star f](-i\omega). \quad \text{(B11)}\end{aligned}$$

Thus, we arrive at the following expression for the energy splitting to second order in J:

$$\begin{aligned}\delta E_0 &= Jh\rho_0 h + \frac{J^2}{4}(\chi^{+-} - \chi^{-+}) \\ &= Jh\rho_0 + \frac{J^2}{4}\int \frac{d\omega}{2\pi}\frac{\mathrm{Tr}[g_s \star g_t](i\omega)}{i\omega}. \end{aligned} \quad \text{(B12)}$$

As discussed in the main text, this expression vanishes as $h \to 0$ due to the vanishing (odd-frequency) triplet correlations described by $g_t \propto h \to 0$.

APPENDIX C: LOGARITHMIC DIVERGENCE

In this Appendix, we explicitly show that the expression for the energy splitting depends logarithmically on the ratio of the bandwidth to the gap. It turns out that this can be most conveniently shown by performing the integral over imaginary time τ using Eq. (A17). Let us recall that $s_0^+ = c_{0\uparrow}^\dagger c_{0\downarrow}$ and $s^- = c_{0\downarrow}^\dagger c_{0\uparrow}$. For the calculation of the correlation functions,

$$\mathcal{C}^{+-}(\tau) = -\langle \mathcal{T}[s_0^+(\tau)s_0^-(0)]\rangle, \quad \text{(C1)}$$

$$\mathcal{C}^{-+}(\tau) = -\langle \mathcal{T}[s_0^-(\tau)s_0^+(0)]\rangle, \quad \text{(C2)}$$

using Wick's theorem, we need the local correlation functions for spin-up and -down single-particle excitations, whose Fourier transform is displayed in Eq. (B5). Computing their inverse Fourier transforms in imaginary time for $T = 0$, we find

$$\begin{aligned}\mathcal{G}^0_{\alpha_\sigma}(\tau) &= -\left\langle \mathcal{T}\left\{\begin{pmatrix} c_{0\sigma}(\tau) \\ c^\dagger_{0,-\sigma}(\tau)\end{pmatrix} \otimes [c^\dagger_{0\sigma}(0) \quad c_{0,-\sigma}(0)]\right\}\right\rangle \\ &= -\pi\rho_0 \int \frac{d\omega}{2\pi} e^{-i\omega\tau}\frac{[(i\omega - \alpha h)\tau^0 + \Delta\tau^x]}{\sqrt{\Delta^2 - (i\omega - \alpha_\sigma h)^2}} \\ &= -\rho_0\Delta e^{-\alpha_\sigma h\tau}[\mathrm{sgn}(\tau)K_1(\Delta|\tau|)\tau^0 \\ &\quad + K_0(\Delta|\tau|)\tau^x], \end{aligned} \quad \text{(C3)}$$

where $\alpha_\uparrow = +1$ and $\alpha_\downarrow = -1$. The last expression in terms of the Bessel K_0 and K_1 functions is valid in the wide band limit where $|\tau| \gg \tau_c$, with $\tau_c \sim D^{-1}$, and D being the bandwidth. Hence, we obtain and introduce the result of Eq. (C3),

$$C^{+-}(\tau) = -\rho_0^2\Delta^2 e^{+2h\tau}\big[K_1^2(\Delta|\tau|) - K_0^2(\Delta|\tau|)\big], \quad \text{(C4)}$$

$$C^{-+}(\tau) = -\rho_0^2\Delta^2 e^{-2h\tau}\big[K_1^2(\Delta|\tau|) - K_0^2(\Delta|\tau|)\big]. \quad \text{(C5)}$$

Therefore, for $|\tau| \gg \tau_c$,

$$\begin{aligned}C^{+-}(\tau) - C^{-+}(\tau) &= -2\rho_0^2\Delta^2\big[K_1^2(\Delta|\tau|) - K_0^2(\Delta|\tau|)\big] \\ &\quad \times \sinh(2h\tau), \end{aligned} \quad \text{(C6)}$$

and, introducing the cut off τ_c at short times, we have

$$\begin{aligned}\chi^{+-} - \chi^{-+} &\simeq -\int_{\tau_c}^{+\infty} d\tau\,[C^{+-}(\tau) - C^{-+}(\tau)] \\ &= 2\rho_0^2\Delta^2\int_{\tau_c}^{+\infty} d\tau\,\big[K_1^2(\Delta\tau) - K_0^2(\Delta\tau)\big]\sinh(2h\tau). \end{aligned} \quad \text{(C7)}$$

Note that this expression makes sense only if $|h| < \Delta$, which is the requirement for stability of the spin-split superconductor. Next, we show that this expression is logarithmic divergent in the limit where $\tau_c \to 0$. To see this, let us recall that for small argument $u = \Delta\tau$,

$$K_0(u) = -\ln(u/2) - \gamma + O[u^2\ln(u)], \quad \text{(C8)}$$

$$K_1(u) = \frac{1}{u} + O[u\ln(u)], \quad \text{(C9)}$$

where γ is Euler's constant. Thus, we see that the term involving $K_1^2(\Delta\tau)$ is most singular and behaves as $\sim\tau^{-1}$ as $\tau \to 0$, which means that the above integral

$$\begin{aligned}\chi^{+-} - \chi^{-+} &\simeq \rho_0^2\Delta^2\int_{\tau_c}^{1/\Delta} d\tau\,\frac{4h}{\Delta^2\tau} + \text{regular terms} \\ &= 4\rho_0^2 h\ln\left(\frac{D}{c\Delta}\right) + \text{regular terms}, \end{aligned} \quad \text{(C10)}$$

where we have set $\tau_c = c/D$, where $c \sim 1$ is a constant to be specified below. The (regular) contribution from the anomalous diagram in the limit where $h/\Delta \ll 1$ can be expressed in terms of the integral,

$$\begin{aligned}&\int_{\tau_c\Delta}^{+\infty} du K_0^2(u)\sinh\left(\frac{2h}{\Delta}u\right) \\ &= \frac{2h}{\Delta}\int_{\tau_c\Delta}^{+\infty} du\, uK_0^2(u) + O\left(\frac{h^2}{\Delta^2}\right) = \frac{h}{\Delta} + O\left(\frac{h^2}{\Delta^2}\right), \end{aligned} \quad \text{(C11)}$$

where we have taken the (wide band) limit where $\tau_c\Delta \sim \Delta/D \to 0$ and used $\int_0^{+\infty} du\, uK_0^2(u) = \frac{1}{2}$.

Thus, for small h, we find that the energy shift takes the form

$$\delta E_0 = J\rho_0 h + (J\rho_0)^2 h\left[\ln\left(\frac{D}{c\Delta}\right) - \frac{1}{2}\right] + O(J^3, h^2). \tag{C12}$$

We can set the freedom to define the imaginary-time cutoff τ_c in terms of D^{-1} and choose $c = e^{-1/2}$ in order to absorb the anomalous contribution into the logarithm, which yields the following results quoted in the main text:

$$\delta E_0/h = J\rho_0 + (J\rho_0)^2 \ln\left(\frac{D}{\Delta}\right) + O(J^3, h). \tag{C13}$$

APPENDIX D: PERTURBATION THEORY FOR THE TWO-SITE MODEL

For $J = 0$, the ground state of a two-site model can be obtained by diagonalizing the following two-site quadratic Hamiltonian:

$$H_0 = \sum_{j=0,1} [\Delta(c_{j\uparrow}^\dagger c_{j\downarrow}^\dagger + \text{H.c.}) - h(c_{j\uparrow}^\dagger c_{j\uparrow} - c_{j\downarrow}^\dagger c_{j\downarrow})] - t\sum_\sigma (c_{0\sigma}^\dagger c_{1\sigma} + \text{H.c.}). \tag{D1}$$

To this end, it is convenient to rewrite the Hamiltonian in the basis of bonding and antibonding orbitals described by the operators,

$$c_{\pm,\sigma} = \frac{1}{\sqrt{2}}(c_{0\sigma} \pm c_{1\sigma}), \tag{D2}$$

and thus,

$$H_0 = \sum_{l=\pm} \Delta(c_{l\uparrow}^\dagger c_{l\downarrow}^\dagger + \text{H.c.}) - h(c_{l\uparrow}^\dagger c_{l\uparrow} - c_{l\downarrow}^\dagger c_{l\downarrow}) - t\sum_{\sigma=\uparrow,\downarrow} (c_{+\sigma}^\dagger c_{+\sigma} - c_{-\sigma}^\dagger c_{-\sigma}). \tag{D3}$$

This Hamiltonian can be diagonalized through the following Bogoliubov transformation:

$$\begin{aligned} \gamma_{\pm\uparrow} &= u_\pm c_{\pm\uparrow} - v_\pm c_{\pm\downarrow}^\dagger, \\ \gamma_{\pm\downarrow} &= u_\pm c_{\pm\downarrow} + v_\pm c_{\pm\uparrow}^\dagger, \end{aligned} \tag{D4}$$

where

$$u_+ = \frac{t + \sqrt{t^2+\Delta^2}}{\Delta\sqrt{1 + \left(\frac{t+\sqrt{t^2+\Delta^2}}{\Delta}\right)^2}}, \tag{D5}$$

$$v_+ = -\frac{1}{\sqrt{1 + \left(\frac{t+\sqrt{t^2+\Delta^2}}{\Delta}\right)^2}}, \tag{D6}$$

$$u_- = \frac{-t + \sqrt{t^2+\Delta^2}}{\Delta\sqrt{1 + \left(\frac{-t+\sqrt{t^2+\Delta^2}}{\Delta}\right)^2}}, \tag{D7}$$

$$v_- = -\frac{1}{\sqrt{1 + \left(\frac{-t+\sqrt{t^2+\Delta^2}}{\Delta}\right)^2}}. \tag{D8}$$

The ground state is given by

$$|\text{GS}_m\rangle = |\text{BCS}\rangle\left|m = \pm\tfrac{1}{2}\right\rangle, \tag{D9}$$

where $|\text{BCS}\rangle = |\text{BCS}\rangle_+|\text{BCS}\rangle_-$, with $|\text{BCS}\rangle_\pm = u_\pm|0\rangle_\pm - v_\pm c_{\pm\downarrow}^\dagger c_{\pm\uparrow}^\dagger|0\rangle_\pm$. The first-order energy correction is given by Eq. (13) in Sec. IV. The second-order correction is defined in Eqs. (9) and (11). Using

$$s_0^\pm|\text{BCS}\rangle = \mp\lambda|t_{\pm1}\rangle, \tag{D10}$$

where $\lambda = \frac{1}{2}(u_+v_- - v_+u_-)$, and $|t_{\pm1}\rangle$ are the spin-triplet states in Eq. (17), we arrive at Eq. (18) of the main text.

APPENDIX E: DETAILS OF THE NRG CALCULATIONS

Considering only the s-wave scattering channel, the Hamiltonian in Eq. (1) can be represented as a (Wilson chain) one-dimensional lattice using the adaptive scheme introduced in Ref. [68] for a constant density of states, $\rho(\epsilon) = 1/(2D)$, in the interval $[-D, D]$. The discretization parameter is taken to be $\Lambda = 2$. This procedure yields the following Wilson chain Hamiltonian:

$$H = \sum_{i\geqslant 0} t_i[f_{i,\sigma}f_{i+1,\sigma}^\dagger + \text{H.c.}] + \Delta[f_{i\uparrow}^\dagger f_{i\downarrow}^\dagger + \text{H.c.}] + h[f_\uparrow^\dagger(i)f_\uparrow(i) - f_\downarrow^\dagger(i)f_\downarrow(i)] + J\boldsymbol{S}\cdot\boldsymbol{s}(0) + \frac{Jh}{2D}S^z, \tag{E1}$$

where the hopping decays exponentially as $t_N \sim \Lambda^{-N/2}$. Notice that the pairing potential term does not conserve the particle number. To render the computation more efficient, we follow the method described in Ref. [43] and apply a Bogoliubov transformation,

$$b_{i,\uparrow}^\dagger = \frac{1}{\sqrt{2}}(f_{i,\uparrow}^\dagger + f_{i,\downarrow}), \tag{E2}$$

$$b_{i,\downarrow} = \frac{1}{\sqrt{2}}(f_{i,\uparrow}^\dagger - f_{i,\downarrow}), \tag{E3}$$

followed by a particle-hole transformation,

$$c_{2i,\uparrow}^\dagger = b_{2i,\uparrow}^\dagger, \tag{E4}$$

$$c_{2i,\downarrow} = b_{2i,\downarrow}, \tag{E5}$$

$$c_{2i-1,\uparrow}^\dagger = b_{2i-1,\downarrow}, \tag{E6}$$

$$c_{2i-1\downarrow} = -b_{2i-1,\uparrow}^\dagger. \tag{E7}$$

Thus, we arrive at the following model:

$$H = \sum_{i\geqslant 0}\left\{t_i\sum_\sigma (c_{i,\sigma}c_{i+1,\sigma}^\dagger + \text{H.c.}) + \Delta(-1)^i Q_i^z + 2hs_i^z\right\} + J\boldsymbol{S}\cdot\boldsymbol{s}_0 + \frac{Jh}{2D}S^z. \tag{E8}$$

To reduce the size of the matrices required to diagonalize, the NRG is applied using the following conserved U(1) quantities (Q^z, S_T^z):

$$Q^z = \sum_i Q_i^z = \sum_i [n_{i,\uparrow} + n_{i,\downarrow} - 1], \tag{E9}$$

$$S_T^z = S^z + \sum_i s^z(i) = S^z + \frac{1}{2}\sum_i [n_{i,\uparrow} - n_{i,\downarrow}], \tag{E10}$$

which is suitable for the case with external magnetic fields. At each iteration, we keep at least 1024 states and discard the states above the energy scale $\omega \approx 10\omega_N = 10\Lambda^{(1-N)/2}$. In the presence of the (superconducting) gap, the NRG iteration must be truncated at iterations with energy scale $\omega_N \ll \Delta$ [69]. Thus, we stop our NRG computation at iterations with energy scale $\sim 10^{-5}\Delta$, which is sufficient to accurately obtain the spectral properties. We set the temperature $T \ll \Delta$ so effectively that we can consider our results to be in the zero-temperature limit. For the Kondo model, the spectral weights, $W_\sigma(\epsilon)$, are defined using the T matrices [65]. The spectral weight reads

$$W_\sigma(\epsilon) = -\frac{1}{\pi}\mathrm{Im}\, C_\sigma^R(\epsilon), \tag{E11}$$

$$C_\sigma^R(\epsilon) = \int dt\, e^{i\epsilon t} C_\sigma^R(t), \tag{E12}$$

$$C_\sigma^R(t) = -i\theta(t)\langle\{O_\sigma(t), O_\sigma^\dagger(0)\}\rangle, \tag{E13}$$

where $O_\sigma = [f_{0\sigma}, H_K]$ with $H_K = J\boldsymbol{S}\cdot\boldsymbol{s}_0$. Note that $f_{0\sigma}$ is the operator in the original fermion basis of the superconducting model. To carry out the computation, we obtain the spectral weights using the full density matrix scheme described in Ref. [70] and broaden the discrete data set using a hybrid kernel. The spectral function $A_\sigma(\omega)$ is thus computed from the following expression:

$$\begin{aligned} A_\sigma(\omega) = \sum_\epsilon W_\sigma(\epsilon)\{&\Theta(\epsilon)[\Theta(\epsilon - \epsilon_{\mathrm{gap}}^+) lG(\omega,\epsilon,a) \\ &+ \Theta(\epsilon_{\mathrm{gap}}^+ - \epsilon)G(\omega,\epsilon,b)] \\ &+ \Theta(-\epsilon)[\Theta(\epsilon_{\mathrm{gap}}^- - \epsilon) lG(\omega,\epsilon,a) \\ &+ \Theta(\epsilon - \epsilon_{\mathrm{gap}}^-)G(\omega,\epsilon,b)]\}, \end{aligned} \tag{E14}$$

where

$$lG(\omega,\epsilon,a) = \frac{\Theta(\omega\epsilon)}{a|\omega|\sqrt{\pi}}\mathrm{Exp}\left[-\left(\frac{\ln(|\omega|) - \ln(|\epsilon|)}{a} - \frac{a}{4}\right)^2\right], \tag{E15}$$

$$G(\omega,\epsilon,b) = \frac{1}{b\sqrt{\pi}}\mathrm{Exp}\left[-\left(\frac{\epsilon-\omega}{b}\right)^2\right]. \tag{E16}$$

$\epsilon_{\mathrm{gap}}^+$ and $\epsilon_{\mathrm{gap}}^-$ are the positions of the BCS gap at positive and negative sides. They are determined from the data of the spectral weights. Outside the gap, we use a logarithmic mesh binning ~500 points per decade with respect to the gap and a log-Gaussian kernel with a narrow broadening parameter, $a = 0.2$. Inside the gap, we accumulate all the spectral weights and broaden the weights using a Gaussian kernel with width $b = \Delta/1000$. To eliminate the oscillatory artifacts in the continuum due to discretization, the spectral functions are z-averaged [71] using 16 z-points spanning the interval $[1/16, 1]$.

[1] A. Y. Kitaev, Unpaired Majorana fermions in quantum wires, Phys. Usp. **44**, 131 (2001).

[2] S. Nadj-Perge, I. K. Drozdov, J. Li, H. Chen, S. Jeon, J. Seo, A. H. MacDonald, B. A. Bernevig, and A. Yazdani, Observation of Majorana fermions in ferromagnetic atomic chains on a superconductor, Science **346**, 602 (2014).

[3] M. Ruby, F. Pientka, Y. Peng, F. von Oppen, B. W. Heinrich, and K. J. Franke, End states and subgap structure in proximity-coupled chains of magnetic adatoms, Phys. Rev. Lett. **115**, 197204 (2015).

[4] C. Beenakker, Search for Majorana fermions in superconductors, Annu. Rev. Condens. Matter Phys. **4**, 113 (2013).

[5] S. D. Sarma, M. Freedman, and C. Nayak, Majorana zero modes and topological quantum computation, npj Quantum Inf. **1**, 15001 (2015).

[6] A. P. Mackenzie and Y. Maeno, The superconductivity of Sr 2 RuO 4 and the physics of spin-triplet pairing, Rev. Mod. Phys. **75**, 657 (2003).

[7] S. Ran, C. Eckberg, Q.-P. Ding, Y. Furukawa, T. Metz, S. R. Saha, I.-L. Liu, M. Zic, H. Kim, J. Paglione *et al.*, Nearly ferromagnetic spin-triplet superconductivity, Science **365**, 684 (2019).

[8] H. Zhou, L. Holleis, Y. Saito, L. Cohen, W. Huynh, C. L. Patterson, F. Yang, T. Taniguchi, K. Watanabe, and A. F. Young, Isospin magnetism and spin-polarized superconductivity in Bernal bilayer graphene, Science **375**, 774 (2022).

[9] F. S. Bergeret, A. F. Volkov, and K. B. Efetov, Odd triplet superconductivity and related phenomena in superconductor-ferromagnet structures, Rev. Mod. Phys. **77**, 1321 (2005).

[10] F. S. Bergeret, M. Silaev, P. Virtanen, and T. T. Heikkilä, Colloquium: Nonequilibrium effects in superconductors with a spin-splitting field, Rev. Mod. Phys. **90**, 041001 (2018).

[11] M. Eschrig and T. Löfwander, Triplet supercurrents in clean and disordered half-metallic ferromagnets, Nat. Phys. **4**, 138 (2008).

[12] A. Hijano, S. Ilić, M. Rouco, C. González-Orellana, M. Ilyn, C. Rogero, P. Virtanen, T. T. Heikkilä, S. Khorshidian, M. Spies, N. Ligato, F. Giazotto, E. Strambini, and F. S. Bergeret, Coexistence of superconductivity and spin-splitting fields in superconductor/ferromagnetic insulator bilayers of arbitrary thickness, Phys. Rev. Res. **3**, 023131 (2021).

[13] T. Tokuyasu, J. A. Sauls, and D. Rainer, Proximity effect of a ferromagnetic insulator in contact with a superconductor, Phys. Rev. B **38**, 8823 (1988).

[14] J. Linder, A. Sudbø, T. Yokoyama, R. Grein, and M. Eschrig, Signature of odd-frequency pairing correlations induced by a magnetic interface, Phys. Rev. B **81**, 214504 (2010).

[15] J. Linder, T. Yokoyama, A. Sudbø, and M. Eschrig, Pairing symmetry conversion by spin-active interfaces in magnetic

normal-metal–superconductor junctions, Phys. Rev. Lett. **102**, 107008 (2009).
[16] J. S. Moodera, X. Hao, G. A. Gibson, and R. Meservey, Electron-spin polarization in tunnel junctions in zero applied field with ferromagnetic EuS barriers, Phys. Rev. Lett. **61**, 637 (1988).
[17] R. Meservey and P. Tedrow, Spin-polarized electron tunneling, Phys. Rep. **238**, 173 (1994).
[18] E. Strambini, V. N. Golovach, G. De Simoni, J. S. Moodera, F. S. Bergeret, and F. Giazotto, Revealing the magnetic proximity effect in EuS/Al bilayers through superconducting tunneling spectroscopy, Phys. Rev. Mater. **1**, 054402 (2017).
[19] A. Yazdani, B. A. Jones, C. P. Lutz, M. F. Crommie, and D. M. Eigler, Probing the local effects of magnetic impurities on superconductivity, Science **275**, 1767 (1997).
[20] S.-H. Ji, T. Zhang, Y.-S. Fu, X. Chen, X.-C. Ma, J. Li, W.-H. Duan, J.-F. Jia, and Q.-K. Xue, High-resolution scanning tunneling spectroscopy of magnetic impurity induced bound states in the superconducting gap of Pb thin films, Phys. Rev. Lett. **100**, 226801 (2008).
[21] B. W. Heinrich, J. I. Pascual, and K. J. Franke, Single magnetic adsorbates on *s*-wave superconductors, Prog. Surf. Sci. **93**, 1 (2018).
[22] F. von Oppen and K. J. Franke, Yu-Shiba-Rusinov states in real metals, Phys. Rev. B **103**, 205424 (2021).
[23] J. O. Island, R. Gaudenzi, J. de Bruijckere, E. Burzurí, C. Franco, M. Mas-Torrent, C. Rovira, J. Veciana, T. M. Klapwijk, R. Aguado, and H. S. J. van der Zant, Proximity-induced Shiba states in a molecular junction, Phys. Rev. Lett. **118**, 117001 (2017).
[24] R. Žitko, J. S. Lim, R. López, and R. Aguado, Shiba states and zero-bias anomalies in the hybrid normal-superconductor Anderson model, Phys. Rev. B **91**, 045441 (2015).
[25] A. Jellinggaard, K. Grove-Rasmussen, M. H. Madsen, and J. Nygård, Tuning Yu-Shiba-Rusinov states in a quantum dot, Phys. Rev. B **94**, 064520 (2016).
[26] M. Valentini, F. Peñaranda, A. Hofmann, M. Brauns, R. Hauschild, P. Krogstrup, P. San-Jose, E. Prada, R. Aguado, and G. Katsaros, Nontopological zero-bias peaks in full-shell nanowires induced by flux-tunable Andreev states, Science **373**, 82 (2021).
[27] E. J. Lee, X. Jiang, M. Houzet, R. Aguado, C. M. Lieber, and S. De Franceschi, Spin-resolved Andreev levels and parity crossings in hybrid superconductor–semiconductor nanostructures, Nat. Nanotechnol. **9**, 79 (2014).
[28] M. Pita-Vidal, A. Bargerbos, R. Žitko, L. J. Splitthoff, L. Grünhaupt, J. J. Wesdorp, Y. Liu, L. P. Kouwenhoven, R. Aguado, B. van Heck *et al.*, Direct manipulation of a superconducting spin qubit strongly coupled to a transmon qubit, Nat. Phys. **19**, 1110 (2023).
[29] A. Bargerbos, M. Pita-Vidal, R. Žitko, L. J. Splitthoff, L. Grünhaupt, J. J. Wesdorp, Y. Liu, L. P. Kouwenhoven, R. Aguado, C. K. Andersen *et al.*, Spectroscopy of spin-split Andreev levels in a quantum dot with superconducting leads, Phys. Rev. Lett. **131**, 097001 (2023).
[30] R. Pawlak, M. Kisiel, J. Klinovaja, T. Meier, S. Kawai, T. Glatzel, D. Loss, and E. Meyer, Probing atomic structure and Majorana wave functions in mono-atomic Fe chains on superconducting Pb surface, npj Quantum Inf. **2**, 16035 (2016).
[31] S. Jeon, Y. Xie, J. Li, Z. Wang, B. A. Bernevig, and A. Yazdani, Distinguishing a Majorana zero mode using spin-resolved measurements, Science **358**, 772 (2017).
[32] J. F. Steiner, C. Mora, K. J. Franke, and F. von Oppen, Quantum magnetism and topological superconductivity in Yu-Shiba-Rusinov chains, Phys. Rev. Lett. **128**, 036801 (2022).
[33] A. Mishra, P. Simon, T. Hyart, and M. Trif, Yu-Shiba-Rusinov Qubit, PRX Quantum **2**, 040347 (2021).
[34] M. A. Ruderman and C. Kittel, Indirect exchange coupling of nuclear magnetic moments by conduction electrons, Phys. Rev. **96**, 99 (1954).
[35] T. Kasuya, A theory of metallic Ferro- and Antiferromagnetism on Zener's model, Prog. Theor. Phys. **16**, 45 (1956).
[36] K. Yosida, Magnetic properties of Cu-Mn alloys, Phys. Rev. **106**, 893 (1957).
[37] V. M. Galitski and A. I. Larkin, Spin glass versus superconductivity, Phys. Rev. B **66**, 064526 (2002).
[38] N. Y. Yao, L. I. Glazman, E. A. Demler, M. D. Lukin, and J. D. Sau, Enhanced antiferromagnetic exchange between magnetic impurities in a superconducting host, Phys. Rev. Lett. **113**, 087202 (2014).
[39] Y. Lu, I. V. Tokatly, and F. S. Bergeret, Ferromagnetic ordering of magnetic impurities mediated by supercurrents in the presence of spin-orbit coupling, Phys. Rev. B **108**, L180506 (2023).
[40] K. Akkaravarawong, J. I. Väyrynen, J. D. Sau, E. A. Demler, L. I. Glazman, and N. Y. Yao, Probing and dressing magnetic impurities in a superconductor, Phys. Rev. Res. **1**, 033091 (2019).
[41] J. Li, T. Neupert, B. A. Bernevig, and A. Yazdani, Manipulating Majorana zero modes on atomic rings with an external magnetic field, Nat. Commun. **7**, 10395 (2016).
[42] K. G. Wilson, The renormalization group: Critical phenomena and the Kondo problem, Rev. Mod. Phys. **47**, 773 (1975).
[43] Numerical renormalization group study of magnetic impurities in superconductors, J. Phys. Soc. Jpn. **61**, 3239 (1992).
[44] T. Yoshioka and Y. Ohashi, Ground state properties and localized excited states around a magnetic impurity described by the anisotropic *s* - *d* interaction in superconductivity, J. Phys. Soc. Jpn. **67**, 1332 (1998).
[45] T. Yoshioka and Y. Ohashi, Numerical renormalization group studies on single impurity anderson model in superconductivity: A unified treatment of magnetic, nonmagnetic impurities, and resonance scattering, J. Phys. Soc. Jpn. **69**, 1812 (2000).
[46] R. Bulla, T. A. Costi, and T. Pruschke, Numerical renormalization group method for quantum impurity systems, Rev. Mod. Phys. **80**, 395 (2008).
[47] A. V. Balatsky, I. Vekhter, and J.-X. Zhu, Impurity-induced states in conventional and unconventional superconductors, Rev. Mod. Phys. **78**, 373 (2006).
[48] W.-V. van Gerven Oei, D. Tanasković, and R. Žitko, Magnetic impurities in spin-split superconductors, Phys. Rev. B **95**, 085115 (2017).
[49] E. Vecino, A. Martín-Rodero, and A. Levy Yeyati, Josephson current through a correlated quantum level: Andreev states and π junction behavior, Phys. Rev. B **68**, 035105 (2003).
[50] L. Yu, Bound state in superconductors with paramagnetic impurities, Acta Phys. Sin. **21**, 75 (1965).
[51] H. Shiba, Classical spins in superconductors, Prog. Theor. Phys. **40**, 435 (1968).

[52] A. I. Rusinov, Theory of gapless superconductivity in alloys containing paramagnetic impurities, Zh. Eksp. Theor. Fiz. **56**, 2047 (1969) [Sov. Phys. JETP **29**, 1101 (1969)].

[53] X. Hao, J. S. Moodera, and R. Meservey, Thin-film superconductor in an exchange field, Phys. Rev. Lett. **67**, 1342 (1991).

[54] T. T. Heikkilä, M. Silaev, P. Virtanen, and F. S. Bergeret, Thermal, electric and spin transport in superconductor/ferromagnetic-insulator structures, Prog. Surf. Sci. **94**, 100540 (2019).

[55] B. Kochelaev, L. Tagirov, and M. Khusainov, Spatial dispersion of spin susceptibility of conduction electrons in a superconductor, Zh. Eksp. Theor. Fiz. **76**, 578 (1979) [Sov. Phys. JETP **49**, 291 (1979)].

[56] Y. A. Izyumov, Y. N. Proshin, and M. G. Khusainov, Competition between superconductivity and magnetism in ferromagnet/superconductor heterostructures, Phys. Usp. **45**, 109 (2002).

[57] F. Bergeret, A. F. Volkov, and K. Efetov, Spin screening of magnetic moments in superconductors, Europhys. Lett. **66**, 111 (2004).

[58] F. S. Bergeret, A. F. Volkov, and K. B. Efetov, Induced ferromagnetism due to superconductivity in superconductor-ferromagnet structures, Phys. Rev. B **69**, 174504 (2004).

[59] J. A. Andrade and A. M. Lobos, Anisotropy and spin-fluctuation effects on the spectral properties of Shiba impurities, Phys. Rev. B **99**, 054508 (2019).

[60] S. Trivini, J. Ortuzar, K. Vaxevani, J. Li, F. S. Bergeret, M. A. Cazalilla, and J. I. Pascual, Pair excitations of a quantum spin on a proximitized superconductor, Phys. Rev. Lett. **130**, 136004 (2023).

[61] A. Skurativska, J. Ortuzar, D. Bercioux, F. S. Bergeret, and M. A. Cazalilla, Robust spin polarization of Yu-Shiba-Rusinov states in superconductor/ferromagnetic insulator heterostructures, Phys. Rev. B **107**, 224507 (2023).

[62] Note that there is a typographical error in the expression above Eq. (B1) of [61]. The correct expression for the singlet state energy in the single-site model is $\epsilon_1 = -\frac{h+\sqrt{h^2+J^2}}{2}$.

[63] F. S. Bergeret and A. F. Volkov, Triplet odd-frequency superconductivity in hybrid superconductor-ferromagnet structures, Ann. Phys. **456**, 169232 (2023).

[64] A. C. Hewson, *The Kondo Problem to Heavy Fermions*, Cambridge Studies in Magnetism (Cambridge University Press, Cambridge, 1993).

[65] T. A. Costi, Kondo effect in a magnetic field and the magnetoresistivity of Kondo alloys, Phys. Rev. Lett. **85**, 1504 (2000).

[66] This approximation can be justified in the large spin S limit with $S^z = O(S)$ and $S^{\pm} = O(\sqrt{S})$.

[67] G. D. Mahan, *Many Particle Physics*, 3rd ed. (Plenum, New York, 2000).

[68] R. Žitko, Adaptive logarithmic discretization for numerical renormalization group methods, Comput. Phys. Commun. **180**, 1271 (2009).

[69] T. Hecht, A. Weichselbaum, J. von Delft, and R. Bulla, Numerical renormalization group calculation of near-gap peaks in spectral functions of the Anderson model with superconducting leads, J. Phys.: Condens. Matter **20**, 275213 (2008).

[70] A. Weichselbaum and J. von Delft, Sum-rule conserving spectral functions from the numerical renormalization group, Phys. Rev. Lett. **99**, 076402 (2007).

[71] M. Yoshida, M. A. Whitaker, and L. N. Oliveira, Renormalization-group calculation of excitation properties for impurity models, Phys. Rev. B **41**, 9403 (1990).